PERFORMANCE ANALYSIS OF COMPOSITE FADING CHANNELS

A THESIS

SUBMITTED TO THE DELHI TECHNOLOGICAL UNIVERSITY

FOR THE AWARD OF THE DEGREE OF

DOCTOR OF PHILOSOPHY

IN

Electronics and Communication Engineering

SUBMITTED BY

SANDEEP KUMAR

DEPARTMENT OF ELECTRONICS & COMMUNICATION ENGINEERING

DELHI TECHNOLOGICAL UNIVERSITY

DELHI- 110042 (INDIA)

DECEMBER 2018

DELHI TECHNOLOGICAL UNIVERSITY

CERTIFICATE

This is to certify that the thesis entitled **"PERFORMANCE ANALYSIS OF COMPOSITE FADING CHANNELS"** being submitted by Sandeep Kumar (Reg. No.: 2K14/PhD/EC/02) for the award of degree of Doctor of Philosophy to the Delhi Technological University is based on the original research work carried out by him. He has worked under my supervision and has fulfilled the requirements which to my knowledge have reached the requisite standard for the submission of this thesis. It is further certified that the work embodied in this thesis has neither partially nor fully submitted to any other university or institution for the award of any degree or diploma.

Dr. Priyanka Jain
(Supervisor)
Assistant Professor,
Department of ECE,
Delhi Technological University,
Delhi, India

Prof. Sanjay Kumar Soni
(Co-Supervisor)
Department of ECE,
MMMUT Gorakhpur,
Uttar Pradesh, India

ACKNOWLEDGEMENT

As the curtains draw on my journey as a Ph.D. student, and I look forward to embarking on my career, I have many people to thank. Foremost of them is my advisors, Dr. Priyanka Jain and Prof. Sanjay Kumar Soni, without whom this thesis would not have been possible. Their substantial and thorough approach, together with their genuine interest in the research subject, turned my research work into a great experience.

With great pleasure, I express my heartfelt gratitude to Dr. Kuldeep Singh for his advice, numerous suggestions, constructive criticism and constant support throughout the period of my research. I would like to thank Dr. Dinesh Kumar Viswakarma, Mr. Pappu Kumar Verma and Mr. Rahul Bansal for their kind help, fruitful discussions and wisdom. I would also thank my colleagues Mr. Sanjay Motia, Mr. Nitin Sharma and Mr. Gaurav Tripathi for their support in numerous discussion and continuous motivation.

Above all, my heartfelt thanks go to my parents, my daughters (Saanvi and Manaira) and my wife (Manpreet Kaur). I know I wouldn't finish the Ph.D. without their non-stopping love, encouragement and support. I admire my wife’s sincere efforts in providing support at various stages.

Finally, I thank all those who helped and supported me. Thank you so much!

ABSTRACT

The presence of both the fading and shadowing effects (also called composite multipath/shadowed fading) is often encountered in a realistic radio propagation scenario, thus, making it necessary to consider the simultaneous effect of fading and shadowing on the received signal. The performance of *L*-Hoyt/gamma and *L*-Hoyt/lognormal composite fading channels with Maximum Ratio Combining (MRC) employing micro-diversity is analyzed. Closed-form expressions for distribution function, moments, outage probability and channel capacity are derived using the probability density function (PDF) of the received instantaneous signal to noise ratio (SNR) in terms of hypergeometric functions. The detailed analysis of communication system in terms of average bit/symbol error probability (ABEP/ASEP) for both coherent and non-coherent modulation techniques are performed.

The performance of energy detector over *L*-Hoyt/gamma and *L*-Hoyt/lognormal channel is also performed. The analytical expressions of average probability of detection and the average area under the receiver operating characteristic over the composite fading channel are derived. In addition, the optimized threshold has been incorporated to overcome the problem of spectrum sensing (SS) at low signal to noise ratio. For independent diversity receivers the analysis has been carried out for the arbitrary number of input branches. The effect of diversity order and fading parameters on the performance measures are studied. For the expressions with infinite series, the convergence is observed and wherever possible the expressions for upper bound on truncation error have been provided. To validate the accuracy of the derived expressions Monte-Carlo/Exact simulations are performed. The results are useful for system design engineers and can be

directly used in several wireless applications such as cooperative and non-cooperative cognitive radio networks.

LIST OF PUBLICATIONS

1. **Sandeep Kumar,** Sanjay Kr. Soni, Priyanka Jain, "Micro-Diversity Analysis of Error Probability and Channel Capacity over Hoyt/gamma Fading", *Radioengineering*, 2017, vol. 26, no. 4, pp. 1096-1103. DOI: 10.13164/re.2017.1096. (**SCI journal with Impact factor – 1.048**).
2. **Sandeep Kumar,** Sanjay Kr. Soni, Priyanka, "Performance of MRC receiver over Hoyt/lognormal Composite Fading Channel", *International Journal of Electronics*, 2018, vol. 105, no. 9, pp. 1433-1450 DOI: https://doi.org/10.1080/00207217.2018.1460870, (**Taylor & Francis, Impact factor – 0.939**).
3. Rupender Singh, Sanjay Kr. Soni, Ram Shringar Raw, **Sandeep Kumar**, "A New Approximate Closed-Form Distribution and Performance Analysis of a Composite Weibull/lognormal Fading Channel", *Wireless Personal Communications,* 2017, vol. 92, no. 3, pp. 883–900. DOI: https://doi.org/10.1007/s11277-016-3583-3. (**Springer, Impact factor – 1.2**)
4. **Sandeep Kumar,** Pappu Kr. Verma, Manpreet Kaur, Sanjay Kr. Soni, Priyanka Jain, "Performance Evaluation of Energy Detection over Hoyt/gamma Channel with MRC Reception", *Journal of Electromagnetic Waves and Applications*, 2018, vol. 105, no. 9, pp. 1433-1450. DOI: https://doi.org/10.1007/s11277-016-3583-3. (**Taylor & Francis, Impact factor – 0.864**)
5. **Sandeep Kumar,** Sanjay Kumar Soni, Priyanka Jain, "Performance Analysis of Hoyt/lognormal Composite Fading Channel", *IEEE International Conference on*

Wireless Communications Signal Processing and Networking (WiSPNET-2017), Chennai, 2017, pp. 2503-2507. DOI**:** 10.1109/WiSPNET.2017.8300212.

6. Rupender Singh, Sanjay Kr. Soni, Pappu Kr. Verma, **Sandeep Kumar**, "Performance Analysis of MRC Combiner Output in Lognormal Shadowed Fading", *IEEE International Conference on Computing, Communication and Automation (ICCCA-2015),* Noida, 2015, pp. 1116-1120. DOI**:** 10.1109/RAECE.2015.7510236.

TABLE OF CONTENT

LIST OF TABLES

LIST OF FIGURES

LIST OF ACRONYMS

ABEP	average bit error probability
ASEP	average symbol error probability
AUC	area under the receiver operating characteristics curve
AWGN	additive white Gaussian noise
BFSK	binary frequency shift keying
BPF	band-pass filter
CAUC	complementary AUC
CDF	cumulative distribution function
CFD	cyclostationary feature detection
CIFR	channel inversion fixed rate
CR	cognitive radio
CROC	complementary receiver operating characteristics
CSI	channel state information
dB	decibel
DEQPSK	differentially encoded quadrature phase shift keying
DPSK	differential phase shift keying

DQPSK	differential quadrature phase shift keying
EGC	equal gain combining
FSK	frequency shift keying
i. i.d.	independent and identically distributed
IoT	internet of things
LOS	line-of-sight
MFD	matched filtering detection
MFSK	M-ary FSK
MGF	moment generating function
MIMO	multiple-input multiple-output
M-QAM	M-ary quadrature amplitude modulation
MRC	maximal ratio combining
MSE	mean square error
ORA	optimal rate adaptation
PU	primary User
PDF	probability density function
QPSK	quadrature phase shift keying

RF	radio frequency
ROC	receiver operating characteristics
RV	random variable
SC	selection combining
SDR	software-defined radio
SNR	signal-to-noise ratio
SS	spectrum sensing
SU	secondary user
TIFR	truncated CIFR
TWDP	two waves diffused power
UWB	ultra-wideband

LIST OF SYMBOLS

$I_0(.)$	modified Bessel function of first kind and order zero
$\log_e(.)$	natural log
$\log_2(.)$	logarithm with base 2
$\Gamma(.)$	gamma function
$\sum_{i=1}^{N}(.)$	summation
$E[.]$	expectation operator
$\Gamma(a,b)=\int_b^{\infty} t^{a-1}\exp(-t)dt$	upper incomplete gamma function
$Y(a,\mathrm{b})=\int_0^{b} t^{a-1}\exp(-\mathrm{t})dt$	lower incomplete gamma function
${}_1F_1(.;.;.)$	confluent hypergeometric function
$G(.)$	Meijer-G function
$(x)_n$	Pochhammer's symbol
$Q(.)$	Q-function
$C(d,r)$	combination of r objects from a set of d objects

$Q_u(.;.)$	Marcum-Q function of order u
$\exp(.)$	exponential
${}_2F_1(.;.;.)$	hypergeometric function

CHAPTER 1

INTRODUCTION

A signal experiences reflection, diffraction and scattering phenomenon while traveling from transmitter to receiver depending upon the dimensions of the objects which comes in its path [**1**]. Due to which the overall quality of the signal reaches the receiver is degraded and it is termed as fading. Depending upon the distance between the transmitter and receiver, fading is characterized into small-scale fading and large-scale fading. In small-scale fading, the rapid fluctuations in the received signal are experienced when the mobile user moves over a small distance (few wavelengths) [**1**]. The gradual variation in the received signal is experienced in large-scale fading when the mobile user moves over large distances [**2**] [**3**]. This chapter discusses different performance measures to study the wireless communication systems. A brief introduction on SS in CR and test statistics of an energy detector is also presented. In the final section, the main contribution and organization of thesis are elaborated.

1.1 Multipath Fading Models

Small-scale fading is also known as multipath fading. In this phenomenon, multiple replicas of the same transmitted information reach the receiver at different time instances. Due to multipath fading, the overall quality of the signal is degraded [**1**] [**3**] [**3**]. The

variation of fading is very in-deterministic, and hence it is difficult to have an accurate model of fading [**5**]. However, many researchers have given a number of mathematical models for fading channels. These models depend upon the different environments and can be described by different statistical distributions. Some of the common multipath fading models are described below.

Rayleigh

Rayleigh distribution is used to model the communication systems when independent scatters are very large. In Rayleigh distribution, there is no LOS component of the signal present at the receiver and the envelope is the sum of two quadrature Gaussian signals [**3**]. The PDF of Rayleigh is

$$p_Z(z) = \frac{z}{\sigma^2}\exp\left\{-\left(\frac{z^2}{2\sigma^2}\right)\right\}, \qquad z \geq 0 \tag{1.1}$$

The random variable can be modeled as $Z = \sqrt{X^2 + Y^2}$. Here *X* and *Y* are i.i.d RVs following Gaussian distribution with mean and variance as 0 and σ^2.

Nakagami

1. Nakagami-*m*: Nakagami-*m* distribution is used to model ionosphere radio and indoor mobile propagation links [**1**]. The PDF of Nakagami-*m* is

$$p_z(z,\Omega) = \frac{2}{\Gamma(m)}\left(\frac{m}{\Omega}\right)^m z^{2m-1}\exp\left(-\frac{m}{\Omega}z^2\right), \qquad z > 0, m \geq \frac{1}{2} \tag{1.2}$$

   here *m* is shape parameter and Ω is controlling spread parameter of Nakagami-*m*. For *m*=1, the PDF of Nakagami-*m* distribution can be simplified to Rayleigh distribution.

2. Nakagami-*n* (Rice): Rice is used to model propagation path when there exist a strong LOS path component and many random weak components [**1**]. The PDF of Rice is given by [**6**] as

$$p_z(z) = \frac{2(1+K)\exp(-K)z}{\Omega}\exp\left(-\frac{(1+K)}{\Omega}z^2\right) I_0\left(2z\sqrt{\frac{K(1+K^2)}{\Omega}}\right), \quad z \geq 0 \quad (1.3)$$

here X and Y are i.i.d. Gaussian RVs having mean m_1, m_2 and variance σ^2 and $Z = \sqrt{X^2 + Y^2}$. K is Rice factor and is related to Nakagami-*n* fading parameter n by $K = n^2$.

3. Nakagami-*q* (Hoyt): This distribution is used to model the propagation channel with more severe fading conditions [**1**]. Hoyt PDF is given as

$$p_Z(z) = \frac{(1+q^2)z}{q\Omega}\exp\left[-\left(\frac{(1+q^2)^2 z^2}{4q^2\Omega}\right)\right] I_0\left(\frac{(1-q^4)z^2}{4q^2\Omega}\right), \qquad z \geq 0 \qquad (1.4)$$

$Z = \sqrt{X^2 + Y^2}$, where X and Y are i.i.d. Gaussian RVs having zero mean and variance σ_x^2 and σ_y^2 respectively. q is the Hoyt fading parameter, having the value from 0 to 1 and is related to the variance as $q = \sigma_y / \sigma_x$ and $\sigma_y^2 = w \times \left[q^2 / (1+q^2)\right]$.

Weibull

Another important fading distribution which is used to model radio system in 800-900 MHz frequency range is Weibull distribution [**7**] [**8**]with the PDF given as

$$p_Z(z) = c\left(\frac{\Gamma\left(1+\frac{2}{c}\right)}{\Omega}\right)^{\frac{c}{2}} z^{(c-1)}\exp\left[-\left\{\frac{z^2}{\Omega}\Gamma\left(1+\frac{2}{c}\right)\right\}^{\frac{c}{2}}\right], \qquad z \geq 0 \tag{1.5}$$

here c is the Weibull fading parameter. For c = 2, the above PDF becomes Rayleigh distribution.

1.2 Shadowing Models

Since variations due to shadowing occur over relatively large distances, this variation comes under large-scale fading. Large obstacles between the transmitter and receiver like buildings and towers are the main cause of shadowing.

Lognormal

There is a general consensus among the researchers that shadowing can be best modeled in the form of lognormal distribution with PDF given by [**1**]

$$p_Z(z) = \frac{1}{\sigma z\sqrt{2\pi}}\exp\left(-\frac{(\log_e z-\mu)^2}{2\sigma^2}\right) \tag{1.6}$$

where μ is the mean and σ is the standard deviation of RV $\log_e z$. These variables can be expressed in *dB* by $\sigma_{dB} = k\sigma$ and $\mu_{dB} = k\mu$ where $k = 10/\ln(10)$ [**3**] [**8**].

Gamma

Representing shadowing using the lognormal PDF often leads to analytical difficulty in deriving the closed-form expressions when combined with other functions. Gamma

distribution is the most acceptable approximation of lognormal distribution and is most widely used in literature to model shadowing effects [**9**]. The PDF of gamma distribution is given as

$$p_Z(z) = \frac{z^{(m-1)}}{\bar{\gamma}^m \Gamma(m)} \exp\left(-\frac{z}{\bar{\gamma}}\right), \qquad z > 0 \tag{1.7}$$

Here $\bar{\gamma}$ is average received SNR and *m* is shaping parameter.

Inverse Gaussian

Inverse Gaussian distribution is also used to model shadowing because of its closeness with the lognormal PDF [**10**] [**11**]. The PDF of inverse Gaussian distribution is expressed as

$$p_Z(z) = \left(\frac{\lambda}{2\pi z^3}\right)^{1/2} \exp\left\{-\frac{\lambda(z-\mu)^2}{2\mu^2 z}\right\}, \qquad z > 0 \tag{1.8}$$

here μ is the mean and λ is the shape parameter of the distribution. The values of both the parameters are positive [**3**].

1.3 Diversity and Combining Techniques

Diversity is a scheme in which two or more independent communication channels with different characteristics are used to improve the reliability of a message [4]. With the increase in the number of independent branches, the probability that all the branches fade at the same time reduces sharply. Thus diversity techniques stabilize the wireless link

leading to an improvement in link reliability or error rate. The following diversity schemes are used.

Time Diversity

The same signal is transmitted over different time instances separated by the coherent time of the channel [**11**].

Frequency Diversity

The same signal is transmitted through different modulation frequencies separated by the coherent bandwidth of the channel to induce independent fading channels [**11**].

Angle Diversity

Angle diversity requires antenna beam widths that are narrow compared to the transmitted beam width, such that the two beams are oriented towards different portions of the transmitted signal, and thus the signals received via the multiple beams appear to be uncorrelated [**13**].

Spatial Diversity

Spatial diversity is based on reception or transmission via multiple antenna elements along with appropriate signal processing that combines the signals from the various antennas. It is observed that with sufficient spacing between antennas, the fading fluctuations of the received signals are independent of each another [**14**].

Diversity Combining

Diversity combining is a method to mitigate the effect of fading. This technique is employed at the receiver side to improve the received instantaneous SNR. The overall performance of the system improves when different replicas of the message are combined efficiently at the receiver [**1**].

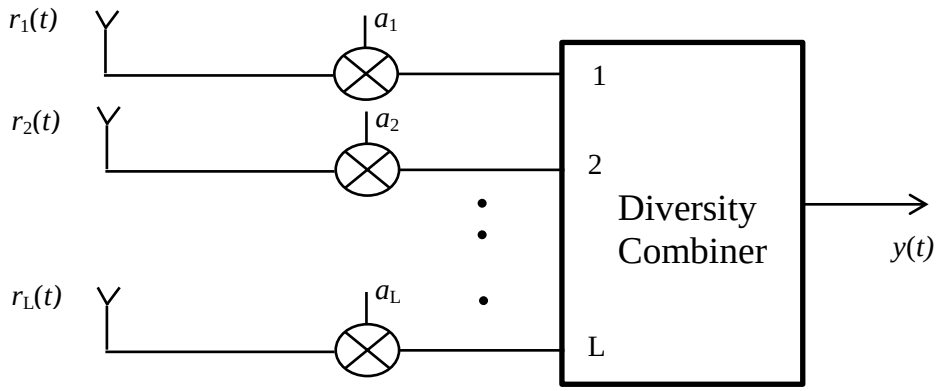

Figure 1.1 Block Diagram of a diversity combining system

The combining may be SC, EGC or MRC. Figure 1.1 is showing a general diversity combiner with *L* independent branches. The output of the combiner is shown in equation 1.9.

$$y(t) = \sum_{l=1}^{L} a_l r_l(t) \tag{1.9}$$

here a_l is the combining coefficient and $r_l(t) = \alpha_l s(t) + n_l(t)$ is the received signal of the l_{th} branch of the combiner.

Selection Combining

In SC, only one signal with the highest SNR is selected out of the *L* available signals at the output of the combiner. From the implementation point of view, this is the simplest scheme out of the available diversity schemes [**3**]. The value of the coefficient is defined in equation 1.10

$$a_l = \begin{Bmatrix} 1, & \max(\gamma_l) \\ 0, & \text{otherwise} \end{Bmatrix} \tag{1.10}$$

Equal Gain Combining

The received signal from all the L branches are co-phased and multiplied with the corresponding weights and added. In EGC equal weights are assigned to all diversity branches. It is suboptimal but simple to implement as it does not depend on channel estimation. The overall SNR at the EGC combiner output is given as [**1**]

$$\gamma = \left(\sum_{l=1}^{L} \alpha_l \right)^2 \frac{E_b}{LN_0} \tag{1.11}$$

where E_b is the energy of the received signal over a bit duration and N_0 is AWGN.

Maximum Ratio Combining

Extension of the selection diversity to linear combining yields the well-known MRC approach. This technique weights the signal received by each diversity branch according to the actual channel estimation, for maximizing the SNR at the output of the combiner. MRC is best of all the combining techniques [**14**] in terms of performance. SNR of the combined signal is given as

$$\gamma = \sum_{l=1}^{L} \gamma_l \tag{1.12}$$

1.4 Performance Measures of the System

There are various measures used in literature for the performance analysis of the communication systems.

Outage Probability

Outage probability is an important performance parameter of a communication system. It is the probability that the received SNR falls below the predetermined threshold(γ_{th}). Mathematically it can be given by [**1**] as

$$P_{out}(\gamma_{th}) = \int_0^{\gamma_{th}} p_\gamma(\gamma)\, d\gamma \tag{1.13}$$

Amount of Fading

The AF is defined as the ratio of the variance to the square mean output SNR. It is used to measure the severity of the channel and can be expressed as [**1**]

$$AF = \frac{E\left[\gamma^2\right]}{E\left[\gamma\right]^2} - 1 \tag{1.14}$$

Channel Capacity

Channel capacity is another performance parameter which is kept in mind while designing the system. Different adaptive transmissions schemes of channel capacity such as ORA, CIFR and TIFR are discussed in this thesis.

ASEP/ABEP

ASEP/ABEP is commonly used to measure the performance of digital communication systems in the fading environments. ASEP/ABEP is defined by [**1**] as

$$\overline{P}_e = E\left[P_e(\gamma)\right] = \int_0^{\infty} P_e(\gamma)\, p_\gamma(\gamma) d\gamma \tag{1.15}$$

here $P_e(\gamma)$ is the instantaneous error probability. $P_e(\gamma)$ depends upon on the modulation technique used in the system.

1.5 Cognitive Radios and Spectrum Sensing

Researchers have found out that the fixed allocation of spectrum causes underutilization of radio spectrum. This is because most of the channels are occupied only for a short period, while these remain unoccupied for rest of the time. Therefore, the problem of lack of RF spectrum is a result of underutilization of the available spectrum [**15**]. To mitigate this problem, CR, inclusive of SDR, has been proposed as a tempting solution to the problem of scarcity of the spectrum [**15**] [**16**] [**17**].

There are two types of users in CR networks: the PUs which are licensed users and the SUs which are unlicensed users. The PU has the higher priority to occupy the particular frequency band whereas the SU has the lower priority for that. The SUs can employ the frequency band of the PU when PU is not using that band. SU should have the capability to sense the presence of the PU in a particular frequency band and make the correct decision in a timely and accurate manner [**18**]. Hence, the SU is equipped with the cognitive capability which is not available in the conventional radio systems [**18**] [**19**].

SS is a crucial part of CR network because all the steps depend on the result of this process. In the open technical literature, many SS techniques are used to detect the presence of PUs signals, such as MFD, CFD, and energy detection. Out of these techniques, energy detection has been widely used to provide SS in both CR and the UWB systems. In contrast to the MFD and the CFD techniques, the energy detection is a non-coherent detection method. Thus, the computational and implementation complexity

of this technique is low in comparison with the aforementioned techniques. Moreover, it needs a shorter time to provide the sensing result [**20**]. In spite of the energy detection technique having the accuracy, high speed, low complexity and low power consumption, new challenges appear when it is used to detect the PU signal in CR networks. Therefore, the designing a good energy detector requires overcoming these challenges. One of these challenges is the difficulty in selecting the threshold value that depends on the noise power and accordingly may change over time [**19**]. The second challenge arises when the wireless signals concurrently undergo multipath fading and shadowing. In spite of few works that have been devoted to deal with this challenge, an extensive study by using a practical channel model should be investigated to get clarifications about the impacts of composite fading on the performance of the energy detector. Another challenge is the complexity of channel models expressions that leads to intractable performance metrics especially when diversity reception schemes are used. This challenge can also be noticed in analyzing the performance of communications systems.

Motivated by these challenges, this thesis studies the behavior of energy detector over different channel models for SS in CR network. Moreover, some techniques are utilized to improve the performance of energy detector under different communication scenarios.

1.6 Test Statistic of an Energy Detector

Consider a narrow band composite signal, $r(t)$ is detected at the receiver. The received signal can be represented by [**21**] as

$$r(t)=\begin{cases} n(t) & ;H_0 \\ h*s(t)+n(t) & ;H_1 \end{cases} \tag{1.16}$$

here *h* denotes the time-invariant channel gain, $s(t)$ denotes the unknown deterministic signal coming from the transmitter and $n(t)$ is AWGN.

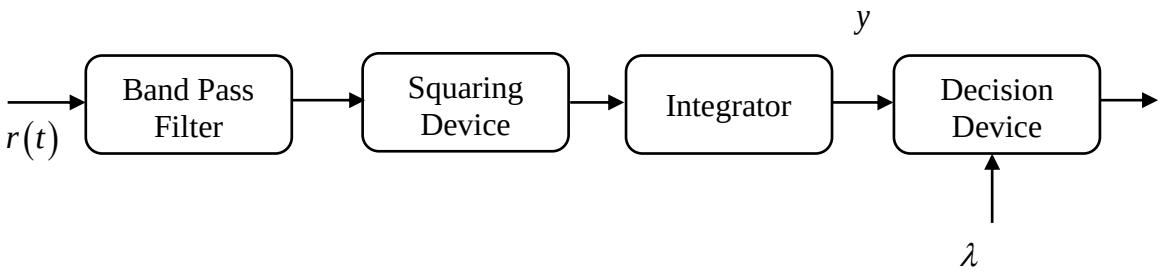

Figure 1.2 Block diagram of an energy detector

As shown in Figure 1.2, $r(t)$ is passed through a BPF, squaring device and integrator. The output of the integrator, *y* acts as the test statistic. The decision device compares *y* with the predefined threshold (λ). The received signal can be formulated by binary hypothesis H_0(signal is not present) and H_1(signal is present). The output of integrator can be expressed as $y = (2/N_0)\int_0^T r^2(t)dt$. *y* can be expressed by [**21**] as

$$y = (2/N_0)\int_0^T n^2(t)dt = \sum_{k=1}^{2u}\left(n_k / \sqrt{(N_0 B)}\right)^2 : H_0 \tag{1.17}$$

$$y \sim \chi^2_{2u} \tag{1.18}$$

Note that since $n_k \sim N(0, N_0 B)$, *y* under H_0, is the square sum of $2u$ Gaussian random variable with mean 0 and variance 1. Thus *y* is chi-square distribution (central, $2u$ degrees of freedom) and $u = TB$(time-bandwidth product) [**22**]. Similarly, under the alternate hypothesis H_1, the decision statistic is chi-square distribution (non-central, $2u$ degrees of freedom and 2γ non-centrality parameter), and can be expressed by [**21**] as

$$y=\left(2/N_0\right)\int_0^T\left(h*s\left(t\right)+n\left(t\right)\right)^2dt=\sum_{k=1}^{2u}\left(\left(hx_k+n_k\right)/\sqrt{\left(N_0W\right)}\right)^2:H_1 \tag{1.19}$$

$$y\sim{\chi_{2u}}^2\left(2\gamma\right) \tag{1.20}$$

Thus, knowing the PDF of decision statistic *y*, one can easily estimate the probability of *y* being less than λ which is nothing but the outage probability of *y*. The probability of detection, $P_d\left(\gamma,\lambda\right)$ is given by [**23**] as

$$P_d\left(\gamma,\lambda\right)=P_r\left(y>\lambda/H_1\right)=Q_u\left(\sqrt{2\gamma},\sqrt{\lambda}\right) \tag{1.21}$$

and the probability of false alarm, $P_f\left(\lambda\right)$ is given by [**23**] as

$$P_f\left(\lambda\right)=P_r\left(y>\lambda/H_0\right)=\frac{\Gamma\left(u,\frac{\lambda}{2}\right)}{\Gamma\left(u\right)} \tag{1.22}$$

Generalized Marcum-*Q* function can be defined in equation (4.74) of [**1**] as

$$Q_u\left(\sqrt{2\gamma},\sqrt{\lambda}\right)=\sum_{m=0}^{\infty}\exp\left(-\gamma\right)\frac{\gamma^m}{m!}\sum_{l=0}^{m+n-1}\frac{1}{l!}\exp\left(-\frac{\lambda}{2}\right)\left(\frac{\lambda}{2}\right)^l \tag{1.23}$$

Using equation (8.352.2) of [**24**], Marcum-*Q* function can be written in terms of upper incomplete gamma function as

$$Q_u\left(\sqrt{2\gamma},\sqrt{\lambda}\right)=\exp\left(-\gamma\right)\sum_{m=0}^{\infty}\frac{\gamma^m}{m!}\frac{\Gamma\left(m+u,\lambda/2\right)}{\Gamma\left(m+u\right)} \tag{1.24}$$

It is evident from equation 1.21 that $P_f(\lambda)$ is same over any fading channel as it does not depend on the fading parameter. The expression in equation 1.21 and 1.22 are achieved by considering the channel as non-fading, and thus channel gain in equation 1.16 is assumed to be constant. If the channel is characterized by fading channel, then $P_d(\gamma,\lambda)$ in equation 1.21 becomes statistical parameter and hence its average with respect to the given distribution needs to be found.

1.7 Thesis Organization and Contributions

In this thesis, the performance analysis of composite fading channels is performed. The thesis work is divided into different chapters. Chapter wise contribution of the thesis is as follows:

Chapter 2: Literature Review

- A detailed and exhaustive literature survey is presented for the various approaches and techniques used to evaluate the performance of communication systems in different fading channels.
- Performances of various models of energy detector that are widely employed in the literature are given. Based on the literature survey research gaps are identified, and research objective of the thesis is formulated.

Chapter 3: Performance Analysis of *L*-Hoyt/Gamma Composite Fading Channel

- *L*-Hoyt/gamma composite fading channel employing micro-diversity reception using MRC is analyzed.

- The closed-form mathematical expressions for the performance parameters outage probability, AF, channel capacity and ASEP/ABEP are derived.

Chapter 4: Performance Analysis of *L*-Hoyt/Lognormal Composite Fading Channel

- Performance of communications systems with MRC diversity combining schemes over Hoyt/lognormal composite fading channels.
- The analytic expressions of the performance parameters for MRC schemes are provided with high accuracy.

Chapter 5: Energy Detector performance over *L*-Hoyt/Gamma and *L*-Hoyt/Lognormal Composite Fading Channel

- Energy detector performances over L-Hoyt/gamma and L-Hoyt/lognormal channel are presented here. The closed–form mathematical expressions for average probability of detection and average AUC are derived.
- The optimized threshold has been incorporated to overcome the problem of SS at low SNR.

Chapter 6: Conclusion and Future Scope of Work

- Conclusions of proposed methods and algorithms are presented in this chapter.
- A detailed discussion of possible avenues of future scope work is presented.

CHAPTER 2

LITERATURE REVIEW

This chapter presents the summary of various algorithms and methods used to model wireless communication channel and the performance evaluation of these channels present in the literature. A detailed literature review of SS and energy detector performance over different channels are also presented.

2.1 Performance Evaluation of Fading Channels

The propagation of the signal in wireless channels is affected by multipath fading and shadowing [**1**]. There is a general consensus that multipath fading is modeled using the various distribution such as Rayleigh, Nakagami, and Weibull distribution etc. [**1**] [**25**]. Performance measures of these multipath fading models are investigated in the literature. Closed-form expressions of PDF and CDF for the product of *n* independent Rayleigh distributed random variables are derived in [**26**]. Analytical expressions of the performance measures for double Rice channels are obtained in [**27**] while for Bivariate Ricean Model is described in [**28**]. The performance analysis of Weibull distribution is performed in [**29**] [**30**]. In [**29**], second-order statistics and channel capacity for Weibull fading channel are also evaluated.

Hoyt distribution is used to model the small-scale fading characteristics of severely faded wireless systems [**31**]. Analytical expressions for PDF and MGF for Hoyt distribution are obtained in [**1**], and the expression for CDF is derived in [**32**]. The closed-form analysis for the outage probability of Hoyt channel under Rayleigh interference and Rayleigh channel under mixed Rayleigh and Hoyt interference are described in [**33**] [**34**]. The average channel capacity and the ABEP for multi-user MIMO over i.i.d. α–μ distribution are given in [**35**]. A comparison of the ergodic capacity for generalized fading channels is presented in [**30**], while a comparison of second-order statistics for the generalized multipath fading channels is discussed in [**36**].

In shadowed fading, large-scale signal variation can be described in the form of various distributions like lognormal, gamma and inverse Gaussian etc. [**3**]. There is a general consensus that lognormal distribution is the most accurate model of shadowing [**1**]. Error probability over the lognormal fading channel is derived for various modulation schemes in [**37**] [**38**] while its channel capacity is estimated in [**39**]. In [**40**] lognormal fading model is presented and its second order statistics are evaluated. Because of the mathematically simpler form of gamma distribution and its closeness with lognormal, it is most widely used in literature to model shadowing effects [**9**]. Gamma distribution is used in place of lognormal distribution to represent shadowing in *K* [**9**], generalized-*K* [**41**], and Weibull/gamma [**42**] composite distributions. In [**10**], the authors have investigated that inverse Gaussian distribution is better suited for capturing shadowing effect than gamma distribution. So inverse Gaussian distribution is also studied in literature as a model of shadowing. An alternate approach was adopted to represent shadowing and in [**43**], shadowing is modeled by cascading short-term fading, while *N*-

gamma model is suggested in [**44**] to represent shadowing. All the above approaches have their limitations in the sense that none of them can be used in all the scenarios to model shadowing.

Composite fading channels are frequently encountered in the radio wave propagation in which multipath fading is superimposed on shadowing [**1**]. Modeling of composite fading is important in analyzing the wireless communication system such as MIMO and CR network and in the modeling of interference in the cellular system. Various composite fading models such as Rician/lognormal, Rayleigh/lognormal and Nakagami/lognormal are considered, and their performance is demonstrated in [**45**] [**46**] [**47**]. A mixture gamma distribution is studied in [**48**] to find the closed-form expressions for performance parameters of Nakagami/lognormal with high accuracy. In [**49**], considering Weibull/lognormal composite fading, second-order statistics of fading channel have been derived.

However, due to mathematical complexity, the performance parameters of lognormal based composite fading channels are not given in closed-form, which makes the analysis of the channel very difficult [**3**]. The performance of several composite distributions like *K* [**9**] [**50**], generalized-*K* [**41**] and the Weibull/gamma [**42**] have been studied in literature where shadowing is modeled in terms of gamma function. Specifically, in [**51**] a general model of a class of composite fading such as η–μ/gamma is carried out, where the results, as a special case, reduce to Hoyt/gamma case is presented. The channel capacity over composite κ–μ/Nakagami-*m* and κ–μ/gamma channels is studied in [**52**] [**53**] while for α–μ/gamma channel is demonstrated in [**54**]. In [**51**] [**55**], the analytic

expressions for the ABEP, the ergodic capacity and the outage probability for η–μ/gamma fading channels are evaluated.

Performance of Rayleigh/inverse Gaussian composite fading is investigated in [**10**] and the merit of using Rayleigh/inverse Gaussian over *K* channel to represent composite fading is demonstrated. The work in [**11**] model the composite Nakagami/lognormal fading by approximating lognormal shadowing in the form of inverse Gaussian distribution, thus, ensuring the resultant expression in the closed-form. The analysis of various fading and shadowing statistical models are estimated in [**56**].

In [**57**] EGC is used for analyzing the performance of dual-branch Rice and Hoyt fading channel. ABEP performance of both coherent/non-coherent detection for EGC receiver over Hoyt fading is obtained in [**58**] [**59**]. An MGF base approach is used in [**60**] to estimate the performance of EGC over Rice and Hoyt channels. The expressions of the outage probability over α–μ, κ–μ and η–μ channels with EGC receivers with co-channel interference are derived in [**61**]. Performance of SC over Rayleigh [**62**], Nakagami-*m* and Hoyt [**63**] [**64**] fading for the correlated channel is analyzed. MRC is the most popular of all the diversity techniques, and error rate performance of coherent modulation over cascaded Rayleigh fading with receive antenna diversity is investigated in [**65**]. The effect of diversity order on the system performance is also demonstrated. MRC diversity is used for the performance analysis of double Nakagami-*m* fading channels in [**66**] while performance over triple selection diversity is studied in [**67**]. The ergodic capacity of MRC combiner over Hoyt channel is analyzed in [**68**] while ABEP performance is examined in [**69**] [**70**]. The performance of MRC diversity over η–μ fading with co-channel interference is evaluated in [**71**].

Analytic expressions for the ASEP of MRC and EGC schemes for various modulation schemes over α–μ fading channel have been recently studied in [**72**] using Mellin transform. In [**73**] ASEP and the ergodic capacity over i.i.d generalized-*K* fading channels with MRC and SC receivers are computed.

Performance of MRC combiner over lognormal shadowed fading channel is investigated in [**74**]. By using the fact that the sum of lognormal RV is well approximated by another lognormal RV, the ergodic capacity for MRC and EGC over lognormal channel is studied in [**75**]. The effect of cooperative diversity over lognormal channels is demonstrated in [**76**] while dual diversity performance over correlated lognormal channels is analyzed in [**77**].

Short-term fading is mitigated through micro-diversity while the macro-diversity approach is used to overcome the effect of long-term fading. Hinging on the fact that SC diversity enjoys the lowest implementation complexity, the performance of macro-diversity and micro-diversity systems using SC are studied in [**78**] [**79**] [**80**]. In [**78**] [**79**] the first order statistic of the system is examined while in [**80**] second order statistic of the system is evaluated.

2.2 Energy Detection Model and its Performance Evaluation

CR has been suggested as a prompting solution to the spectrum scarcity problem. SS is the key function of CR. In spite of the energy detection technique having the accuracy, high speed and low power consumption, some challenges appear when it is used to sense the PU signal in CR networks. The first challenge is to analyze the behavior of energy

detector in a practical channel model and then propose a method to enhance its performance. The second challenge arises when the wireless signals undergo multipath fading and shadowing. In spite of few works that have been devoted to deal with this challenge, an extensive study by using different channel models should be investigated to get clarifications about the impacts of multipath and shadowing on the energy detector performance.

Energy detector performance over Nakagami-*m* fading channel is studied in [**23**]. The AUC expression of energy detector for Nakagami-*m* and η–μ channels is presented in [**81**]. The analysis of an energy detector under the η–μ fading channel is exploited in [**82**] [**83**]. A generalized expression for the performance of energy detector is derived over α–μ generalized gamma fading model in [**84**] while for κ–μ and κ–μ extreme fading channels are derived in [**85**]. The performance for various SS techniques over TWDP channel has been demonstrated for CR based IoT devices in [**86**].

In a practical wireless communication system, both multipath and shadowing effects are experienced simultaneously. Analysis of energy detection over Rician/lognormal channel is studied in [**87**] while for *K* and generalized-*K* channels is analyzed in [**88**] [**89**]. Energy detection based measures in terms of CROC curves and CAUC curves over Rician/gamma fading channels are discussed in [**90**] and the performance of energy detector over gamma shadowed α–μ, κ–μ and η–μ channels is studied in [**91**].

The analytical expressions for the ROC over Nakagami-*m* channel with diversity combiner is presented in [**92**] while the performance in terms of CROC and CAUC have been derived in [**93**] [**94**]. Based on MGF, energy detector over Nakagmai-*m* and Rician channels in terms of CROC curves with different diversity techniques are studied in [**95**].

An analytical study of SC diversity under η-μ multipath fading is presented in [**96**] while energy detector performance for diversity reception over κ–μ and η–μ channels is proposed in [**97**]. Study of an energy detector over η–μ, κ–μ and α–μ fading with diversity reception is presented in [**98**].

New analytical approach is used in [**99**] to study the energy detector behavior over κ-μ/gamma channel. In [**100**], transmit and relay diversity approaches are used to alleviate the impact of the imperfect reporting channel on the performance of CSS.

In wireless communication systems, energy detector with cooperative SS has been studied over different fading channels. Cooperative SS over κ–μ/gamma channel is analyzed in [**101**]. The performance analysis of cooperative SS is studied over different composite channels [**102**].

Conventional or fixed threshold method does not work at low SNR, the optimized threshold is used in place of the fixed threshold to improve the performance of energy detector [**103**]. In [**104**] [**105**] [**106**], the threshold is optimized for cooperative SS by minimizing the total probability of error over Rayleigh and Nakagami-*m* channel.

2.3 Research Gaps and Motivation

In literature survey, the study for diversity reception of Hoyt fading channel is available, but the micro-diversity analysis of composite Hoyt/gamma and Hoyt/lognormal fading channel has not received enough attention.

There are some challenges in using the energy detector for SS in CR networks that should be addressed to obtain good sensing results. The first challenge is analyzing the behavior of the energy detector in practical channel model without mathematical limitations and

then proposing a method to alleviate the performance of the energy detector by depending on this analysis. The second challenge arises when the wireless signals concurrently undergo multipath fading and shadowing. In spite of few works that have been devoted to deal with this challenge, an extensive study by using a practical channel model should be investigated to get clarifications about the impacts of the composite channel on the performance of the energy detector. Accordingly, an optimal method to alleviate the effects of the shadowing can be developed. Another challenge is the complexity of channel models expressions that leads to intractable performance metrics especially when diversity reception schemes are used. This challenge can also be noticed in analyzing the performance of communication systems.

Motived by these challenges, this thesis studies the performance evaluation of energy detector over the composite channels with diversity combiner in CR network. Moreover, some techniques are utilized for the performance improvement over energy detector under different communication scenarios.

2.4 Problems Formulation

Based on the discussion presented in the previous section, we consider the following problems for analysis in this report. Analysis of diversity receivers over the composite channels with micro-diversity reception can be a potential area of research. The performance evaluation of energy detector over the composite channels with diversity reception can be of interest to the research community.

2.5 Aim and Objectives

The main aim and objectives of this thesis are highlighted in the following points:

- To study the performance of MRC combiner over Hoyt/gamma composite fading channel with the arbitrary number of branches.
- To derive the unified expressions for the performance metrics of communication systems over Hoyt/lognormal composite fading channel for MRC with the arbitrary number of branches.
- To analyze the behavior of the energy detector over Hoyt/gamma composite fading channel with micro-diversity reception using the method which gives non-limited analytic expressions for the performance metrics.
- To study the performance of the energy detector over Hoyt/lognormal composite fading channel with micro-diversity reception that can be applied for a variety of wireless channel models.

To fulfill the above-stated aims and objectives, we focus on the mathematical analysis of the performance measures of the receivers in the best possible compact form.

CHAPTER 3

PERFORMANCE ANALYSIS OF *L*-HOYT/GAMMA COMPOSITE FADING CHANNEL

This chapter demonstrates the performance analysis of *L*-Hoyt/gamma composite fading channel. Hoyt distribution is used to model the short-term fading characteristics of the channel with more severe fading conditions and gamma distribution is the most acceptable approximation of lognormal distribution and is most widely used in literature to model shadowing effects. Short-term fading is mitigated through micro-diversity while the macro-diversity approach is used to overcome the effect of long-term fading. Hinging on the fact that MRC gives the best performance of all the diversity techniques, the composite fading channel employing micro-diversity reception is studied. Closed-form mathematical expressions for distribution function, moments, outage probability and channel capacity are presented in terms of hypergeometric functions. Further, the expressions of ASEP/ABEP for coherent and non-coherent modulation techniques involving *Q*-functions and Marcum-*Q* function are derived over the composite fading channel.

3.1 System and Channel Model

PDF of γ for conditional Hoyt fading channel at the output of *L* branch MRC receiver is defined by [**69**] as

$$p_\gamma(\gamma/w)=\left(\frac{1+q^2}{2qw}\right)^L \frac{\exp\left[-\left(\frac{\left(1+q^2\right)\gamma}{2q^2w}\right)\right]}{\Gamma(L)}\gamma^{(L-1)}{}_1F_1\left(\frac{L}{2};L;\frac{\left(1-q^4\right)\gamma}{2q^2w}\right),\gamma\geq 0 \tag{3.1}$$

where w is the average received SNR of the conditional Hoyt distribution. If w is slowly varying, the PDF in equation 3.1 becomes a statistical term and its average need to be computed. Here, the slowly varying fading is modeled using gamma distribution with PDF given by equation 1.7. The composite fading distribution can be evaluated by using

$$p_\gamma(\gamma)=\int_0^\infty p_\gamma(\gamma/w)\,p_w(w)\,dw \tag{3.2}$$

Substituting equation 1.7 and 3.1 into equation 3.2, we get

$$\begin{aligned} p_\gamma(\gamma)=\int_0^\infty &\left(\frac{1+q^2}{2qw}\right)^L \frac{\exp\left[-\left(\frac{\left(1+q^2\right)\gamma}{2q^2w}\right)\right]\gamma^{(L-1)}}{\Gamma(L)} \\ &\times {}_1F_1\left(\frac{L}{2};L;\frac{\left(1-q^4\right)\gamma}{2q^2w}\right)\frac{w^{(m-1)}}{\bar{\gamma}^m\Gamma(m)}\exp\left(-\frac{w}{\bar{\gamma}}\right)dw \end{aligned} \tag{3.3}$$

where ${}_1F_1(.;.;.)$ can be simplified using equation (9.210.1) of [**24**]. Transforming each exponential term by using equation (07.34.03.0228.01) of [**107**] and rearranging the terms, equation 3.3 can be written as

$$p_\gamma(\gamma)=\sum_{n=0}^\infty \frac{s^L t^n \gamma^{(L+n-1)}\left(\frac{L}{2}\right)_n}{\Gamma(L+n)\Gamma(m)\bar{\gamma}^m n!}\int_0^\infty w^{(m-L-n)-1}G_{0,1}^{1,0}\left[\frac{s\gamma}{qw}\middle|0\right]G_{0,1}^{1,0}\left[\frac{w}{\bar{\gamma}}\middle|0\right]dw \tag{3.4}$$

where $s=\left(1+q^2\right)/2q, t=\left(1-q^4\right)/2q^2$. Using equation (9.31.2) of [**24**], equation (07.34.21.0011.01) of [**107**] and after some mathematical manipulations, the mathematical expression of PDF of *L*-Hoyt/gamma channel can be simplified as

$$p_\gamma\left(\gamma\right)=\sum_{n=0}^{\infty}\frac{t^n\left(\frac{L}{2}\right)_n q^{(n+L-m)}\gamma^{m-1}}{\Gamma\left(L+n\right)\Gamma\left(m\right)\overline{\gamma}^m n! s^{n-m}}G_{0,2}^{2,0}\left[\frac{s\gamma}{q\overline{\gamma}}\middle| 0, n+L-m\right] \tag{3.5}$$

By putting q=1 in the definition of s and t, equation 3.5 can be simplified to PDF of *K* distribution.

3.2 Performance Parameters

3.2.1 Outage Probability

Substituting equation 3.5 in 1.13, the expression for outage probability of *L*-Hoyt/gamma channel comes out as

$$P_{out}\left(\gamma_{th}\right)=\sum_{n=0}^{\infty}\frac{t^n\left(\frac{L}{2}\right)_n q^{(n+L-m)}}{\Gamma\left(L+n\right)\Gamma\left(m\right)n! s^{n-m}}\left(\frac{\gamma_{th}}{\overline{\gamma}}\right)^m G_{1,3}^{2,1}\left[\frac{s\gamma_{th}}{q\overline{\gamma}}\middle| \begin{matrix}1-m\\ 0, n+L-m, -m\end{matrix}\right] \tag{3.6}$$

3.2.2 Amount of Fading

The i^{th} moment of γ is defined as $E\left[\gamma^i\right]=\int_0^\infty \gamma^i p_\gamma\left(\gamma\right)d\gamma$. By putting equation 3.5 in the definition and using equation (07.34.21.0009.01) of [**107**], the i^{th} moment of the composite fading channel can be easily evaluated as

$$E\left[\gamma^{i}\right]=\sum_{n=0}^{\infty}\frac{t^{n}\left(\frac{L}{2}\right)_{n}q^{(n+L+i)}\overline{\gamma}^{i}}{\Gamma(L+n)\Gamma(m)n!s^{n+i}}\left[\Gamma(m+i)\right]\left[\Gamma(n+L+i)\right] \tag{3.7}$$

The AF is defined as $AF=E\left[\gamma^{2}\right]/E\left[\gamma\right]^{2}-1$. AF of the *L*-Hoyt/gamma channel can be easily evaluated using equation 3.7.

3.2.3 Channel Capacity

Shannon's channel capacity is defined as the maximum rate of data transmission over a channel with small error probability. It is an important performance parameter which is kept in mind while designing the system. Motivated by this fact, the closed-form expressions for channel capacity under ORA and CIFR are presented here.

3.2.3.1 ORA

In this scheme, the transmit power remains constant. This scheme is more practical and its channel capacity is expressed by [**1**] as

$$C_{ora}=B\int_{0}^{\infty}\log_{2}(1+\gamma)p_{\gamma}(\gamma)d\gamma \tag{3.8}$$

here *B* is the band-width of the channel. Putting equation 3.5 in 3.8, and using equations (07.34.03.0456.01) and (07.34.21.0011.01) of [**107**], the above equation can be simplified as

$$\frac{C_{ora}}{B}=\sum_{n=0}^{\infty}\frac{t^{n}\left(\frac{L}{2}\right)_{n}q^{(n+L-m)}}{\Gamma(L+n)\Gamma(m)\overline{\gamma}^{m}n!s^{n-m}}G_{2,4}^{4,1}\left[\frac{s}{q\overline{\gamma}}\middle|\begin{matrix}-m,1-m\\0,n+L-m,-m,-m\end{matrix}\right] \tag{3.9}$$

3.2.3.2 CIFR

Under this policy, transmitter allocates higher power to the channel with low SNR and lower power to channel with higher SNR such that the constant received power is maintained. It is the capacity which gives lower bound of data rate through any channel. The channel capacity under this scheme is defined by [**1**] as

$$C_{cifr} = B\log_2\left(1+\frac{1}{\int_0^{\infty} p_\gamma(\gamma)/\gamma d\gamma}\right) \tag{3.10}$$

Using the result of equation 3.7 for $E[1/\gamma]$ in equation 3.10, one can easily find out the final expression of C_{cifr}.

3.2.4 ASEP/ABEP

In this section, we have derived the closed-form expressions for ASEP/ABEP for coherent/non-coherent detection. The general formula for ASEP/ABEP is given by equation 1.15.

3.2.4.1 Coherent Modulation Scheme

The generalized instantaneous error probability for coherent modulation is given by [**38**]

$$P_e(\gamma) = \sum_{d=1}^{D} \alpha_d \left[Q\left(\sqrt{c_0\gamma}\right)\right]^d \tag{3.11}$$

The values of D, α_d and c_0 depends upon the modulation scheme and their values are defined in Table 3.1. It is difficult to perform the averaging of instantaneous error

probability in equation 1.15 by directly applying equation 3.11 in terms of *Q*-function. Hence we need to find the approximate of *Q*-function. Various approximations of *Q*-function are used in the literature [**38**] [**108**].

Table 3.1 Coherent Modulation schemes incorporating the integral power of Q-functions

Modulation	**D**	c_0	α_d
Binary Antipodal BPSK	1	2	$\alpha_1 = 1$
Binary Orthogonal BPSK	1	1	$\alpha_1 = 1$
QPSK	1	1	$\alpha_1 = 2$
M-PSK	1	$2\sin^2(\pi/M)$	$\alpha_1 = 2$
M-PAM	1	$\frac{6}{M^2-1}$	$\alpha_1 = \frac{2(M-1)}{M}$
M-QAM	2	$\frac{3}{M-1}$	$\alpha_1 = \frac{4(\sqrt{M}-1)}{\sqrt{M}}$, $\alpha_2 = -\frac{4(\sqrt{M}-1)^2}{M}$
DEQPSK	4	1	$\alpha_1 = 4,\ \alpha_2 = -8,$ $\alpha_3 = 8,\ \alpha_4 = -4$

The *Q*-function is approximated using [**38**] as

$$Q\left(\sqrt{t}\right) \approx \frac{a_1}{2}\exp\left(-b_1 t/2\right) + \frac{a_2}{2}\exp\left(-b_1 t\right) \tag{3.12}$$

Here $a_1 = 0.3070,\ a_2 = 0.4389$ and $b_1 = 1.0510.$ ASEP can be found by substituting equation 3.5 and 3.11 into equation 1.15 and using the approximation of *Q*-function as in equation 3.12. The resultant expression is evaluated as

$$\bar{P}_e \approx \sum_{n=0}^{\infty} \frac{t^n \left(\frac{L}{2}\right)_n q^{(n+L-m)}}{\Gamma(L+n)\Gamma(m)\bar{\gamma}^m n! s^{n-m}} \int_0^{\infty} \gamma^{m-1} G_{0,2}^{2,0}\left[\frac{s\gamma}{q\bar{\gamma}}\middle| 0, n+L-m\right] \times \sum_{d=1}^{D} \alpha_d \left[\frac{a_1}{2}\exp\left(-\frac{b_1 c_0 \gamma}{2}\right) + \frac{a_2}{2}\exp\left(-b_1 c_0 \gamma\right)\right]^d d\gamma \tag{3.13}$$

This integral can be solved by expanding the square bracket of the integrand with the help of binomial theorem $(x+y)^n = \sum_{k=0}^{n} C(n,k) x^{n-k} y^k$. Using equations (07.34.03.0228.01) and (07.34.21.0011.01) of [**107**], the generalized closed-form solution of ASEP for all formats of coherent modulation techniques is given by

$$\bar{P}_e \approx \sum_{n=0}^{\infty} \frac{t^n \left(\frac{L}{2}\right)_n q^{(n+L)}}{\Gamma(L+n)\Gamma(m) n! s^n} \sum_{d=1}^{D} \alpha_d \sum_{r=0}^{d} C(d,r) \left(\frac{a_1}{2}\right)^{d-r} \left(\frac{a_2}{2}\right)^r \times G_{2,1}^{1,2}\left[\frac{(d+r) b_1 c_0 q\bar{\gamma}}{2s}\middle| \begin{matrix} 1-m, 1-n-L \\ 0 \end{matrix}\right] \tag{3.14}$$

The next section deals with the average probability of error for non-coherent modulation techniques.

3.2.4.2 Non-coherent Modulation Scheme

In some situations, the phase recovery of the carrier signal cannot be recovered accurately. In that situation, the communication system has to be dependent on non-coherent reception. The popularly used modulation techniques in non-coherent reception are FSK DPSK and DQPSK. In [**108**] [**109**] the mathematical expressions for non-coherent reception have been studied. In this section, we have proposed the closed-form analysis for non-coherent reception over the composite fading with diversity.

a) DPSK: The bit error probability for DPSK (a=1) and BFSK (a=0.5) is given by [**13**] as

$$P_e(\gamma) = \frac{1}{2}\exp(-a\gamma) \tag{3.15}$$

Putting equation 3.5 and 3.15 into equation 1.15, and using the transformation of exponential function into G-function and integral of the product of two G-functions using equation (07.34.21.0011.01) of [**107**], we can obtain the final expression of ABEP for non-coherent DPSK and BFSK modulation schemes as

$$\bar{P}_e = \frac{1}{2}\sum_{n=0}^{\infty} \frac{t^n \left(\frac{L}{2}\right)_n q^{(n+L)}}{\Gamma(L+n)\Gamma(m) n! s^n} G_{2,1}^{1,2}\left[\frac{aq\bar{\gamma}}{s} \middle| \begin{matrix} 1-m, 1-n-L \\ 0 \end{matrix} \right] \tag{3.16}$$

b) MFSK: The instantaneous probability of symbol error for MFSK is given by [**13**] as

$$P_e(\gamma) = \sum_{p=1}^{M-1} C(M-1, p) \frac{(-1)^{p+1}}{p+1} \exp\left(-\frac{p}{p+1}\gamma \right) \tag{3.17}$$

here each symbol of MFSK represents $\log_2 M$ bits. The ASEP expression for MFSK is obtained by substituting equation 3.5 and 3.17 into equation 1.15 and using equations (07.34.03.0228.01) and (07.34.21.0011.01) of [**107**]

$$\bar{P}_e = \sum_{n=0}^{\infty} \frac{t^n \left(\frac{L}{2}\right)_n q^{(n+L)}}{\Gamma(L+n)\Gamma(m) n! s^n} \sum_{p=1}^{M-1} C(M-1, p) \frac{(-1)^{p+1}}{p+1} G_{2,1}^{1,2}\left[\frac{pq\bar{\gamma}}{(p+1)s} \middle| \begin{matrix} 1-m, 1-n-L \\ 0 \end{matrix} \right] \tag{3.18}$$

c) DQPSK: Bit error probability for DQPSK is defined by [**13**] as

$$P_e(\gamma) = Q_1(a\sqrt{\gamma}, b\sqrt{\gamma}) - \frac{1}{2} I_0(ab\gamma) \exp\left(-\frac{a^2+b^2}{2}\gamma\right) \tag{3.19}$$

where $a = \sqrt{2\left(1-1/\sqrt{2}\right)}, b = \sqrt{2\left(1+1/\sqrt{2}\right)}$. Substituting equations 3.5 and 3.19 into equation 1.15 and using the expansion of Marcum-Q function and modified Bessel function [**13**], one can write the resulting expression as

$$\begin{aligned}\bar{P}_e = \int_0^\infty \sum_{n=0}^{\infty} & \frac{t^n \left(\frac{L}{2}\right)_n q^{(n+L-m)} \gamma^{m-1}}{\Gamma(L+n)\Gamma(m)\bar{\gamma}^m n! s^{n-m}} G_{0,2}^{2,0}\left[\frac{s\gamma}{q\bar{\gamma}}\middle| 0, n+L-m\right] \\ & \times \left\{ \exp(-x\gamma) \sum_{k=0}^{\infty} \left(\frac{a}{b}\right)^k \sum_{l=0}^{\infty} \frac{(r\gamma)^z}{l!\Gamma(l+k+1)} - \frac{1}{2}\exp(-x\gamma) \sum_{p=0}^{\infty} \frac{(r\gamma)^{2p}}{(p!)^2} \right\} d\gamma\end{aligned} \tag{3.20}$$

where $x = \frac{a^2+b^2}{2}, r = \frac{ab}{2}$, and $z = 2l+k$. Using equations (07.34.03.0228.01) and (07.34.21.0011.01) of [**107**], we can obtain the final result for ABEP of DQPSK as

$$\begin{aligned}\bar{P}_e = & \sum_{n=0}^{\infty} \frac{t^n \left(\frac{L}{2}\right)_n q^{(n+L)}}{\Gamma(L+n)\Gamma(m) n! s^n} \\ & \times \left\{ \begin{array}{l} \sum_{k=0}^{\infty} \left(\frac{a}{b}\right)^k \sum_{l=0}^{\infty} \frac{(r)^z}{l!\Gamma(l+k+1)} \left(\frac{q\bar{\gamma}}{s}\right)^z G_{2,1}^{1,2}\left[\frac{xq\bar{\gamma}}{s}\middle| \begin{matrix} 1-(z+m), 1-(z+n+L) \\ 0 \end{matrix}\right] \\ -\frac{1}{2} \sum_{p=0}^{\infty} \frac{(r)^{2p}}{(p!)^2} \left(\frac{q\bar{\gamma}}{s}\right)^{2p} G_{2,1}^{1,2}\left[\frac{xq\bar{\gamma}}{s}\middle| \begin{matrix} 1-(2h+m), 1-(2h+n+L) \\ 0 \end{matrix}\right] \end{array} \right\}\end{aligned} \tag{3.21}$$

3.3 Numerical Results and Discussions

The validity of our performance parameters are confirmed in this section. The default value of $\overline{\gamma}$ is taken as unity in all the calculations. Monte-Carlo simulations are also included with 10^7 numbers of samples for generating *L*- Hoyt/gamma composite distribution for validating the accuracy of the derived expressions. The simulation results are in close match with the derived results obtained by keeping enough number of terms in the infinite series.

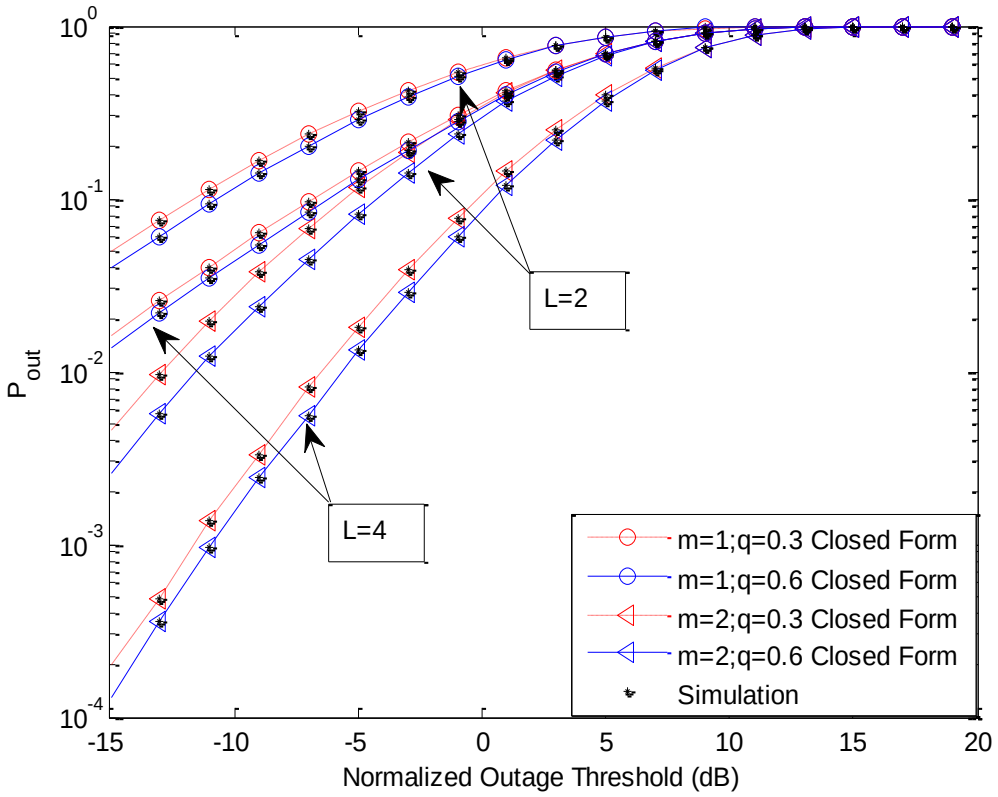

Figure 3.1 Diversity effect on Outage Probability for several values of m and q

In Figure 3.1, outage probability against the normalized outage threshold $(\gamma_{th}/\overline{\gamma})$ for arbitrary values of *m* and *q* using the closed-form expression as given in equation 3.6 is plotted. It is evident from the results that outage probability increases with increase in γ_{th}

indicating an increase in the likelihood of failure to achieve a given threshold level. As expected, the outage probability is shown to decrease with increase in *m* and *q*, hinting an improvement in performance of the receiver. The effect of channel condition improvement with diversity is clearly shown in the plot. AF as a function of *m* for several values of *q* is plotted in Figure 3.2. It is noted that AF decreases as *m* and *L* increases, showing improved performance. Furthermore, as *q* increases, AF plot shift downwards, while it can also be observed that the gap among the curves decreases as *L* increases. Moreover, in Figure 3.3 the impact of *q* on the channel capacity is demonstrated for various values of diversity order *L* based on equation 3.9. It is observed that the increase in the values of *q* or *L* both help to improve the performance of the system.

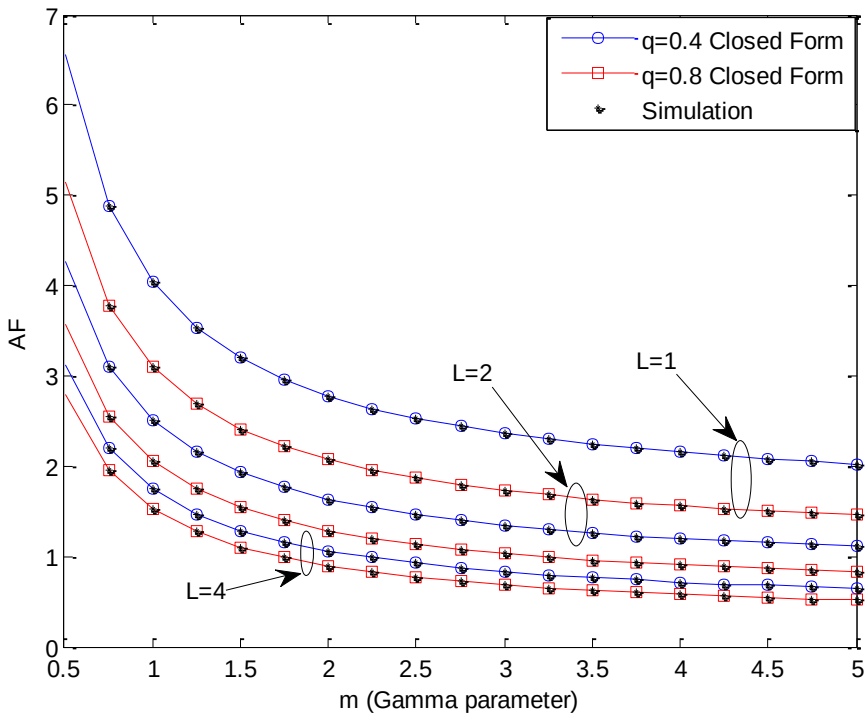

Figure 3.2 AF versus m for several values of q and L

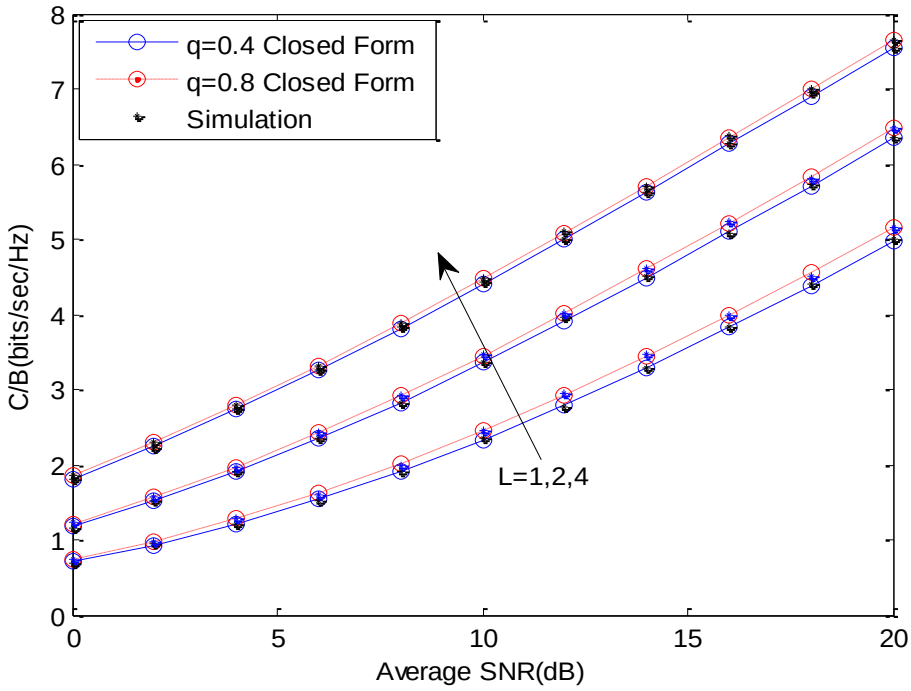

Figure 3.3 Effect of diversity and fading parameter on channel capacity with ORA for m= 1

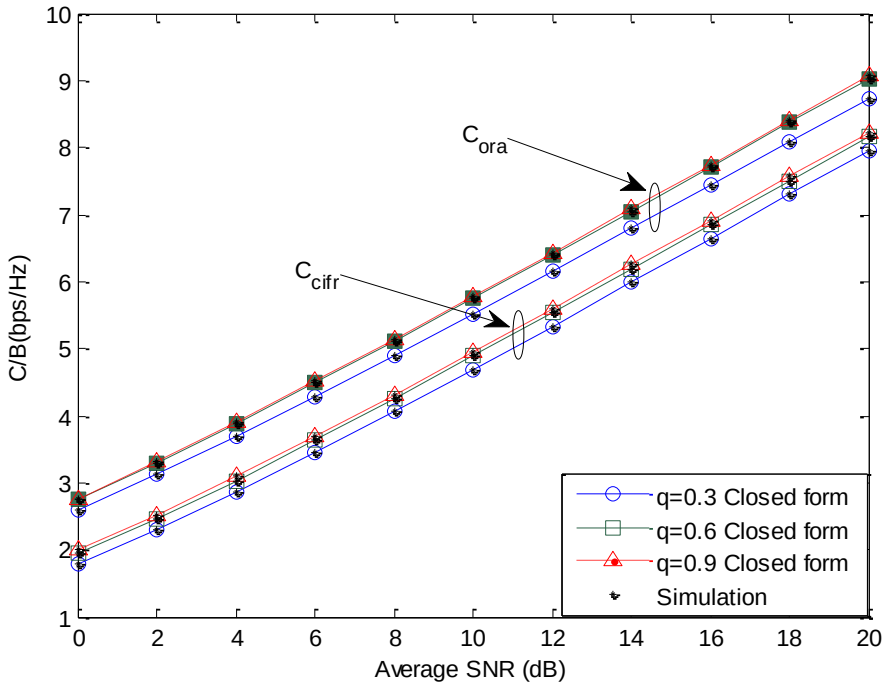

Figure 3.4 Channel Capacity with ORA and CIFR for m= 2 and L= 4

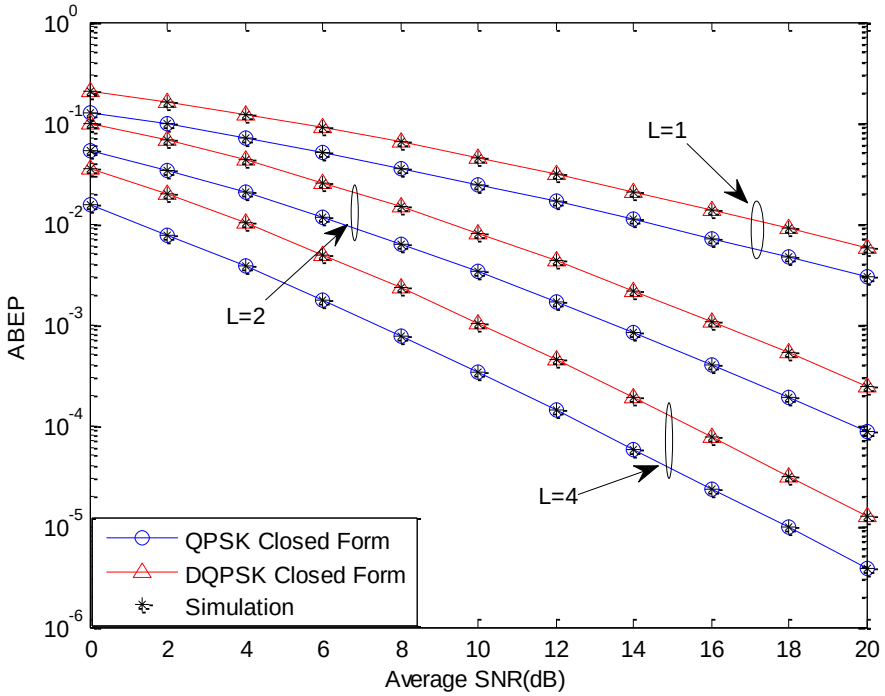

Figure 3.5 ABEP Comparison between QPSK and DQPSK for different values of L

Figure 3.4 depicts the average channel capacity as a function of the average received SNR for the ORA and CIFR schemes with several values of the fading parameter *q*. Monte-Carlo simulations exactly match with the analytical results. It is evident that, as the average received SNR increases, the capacity of both the transmission schemes increases. It is noted that CIFR achieves the lower capacity than ORA. The reason for this is that CIFR uses a fixed transmission data rate; and more power is required to compensate for the effect of severe fading.

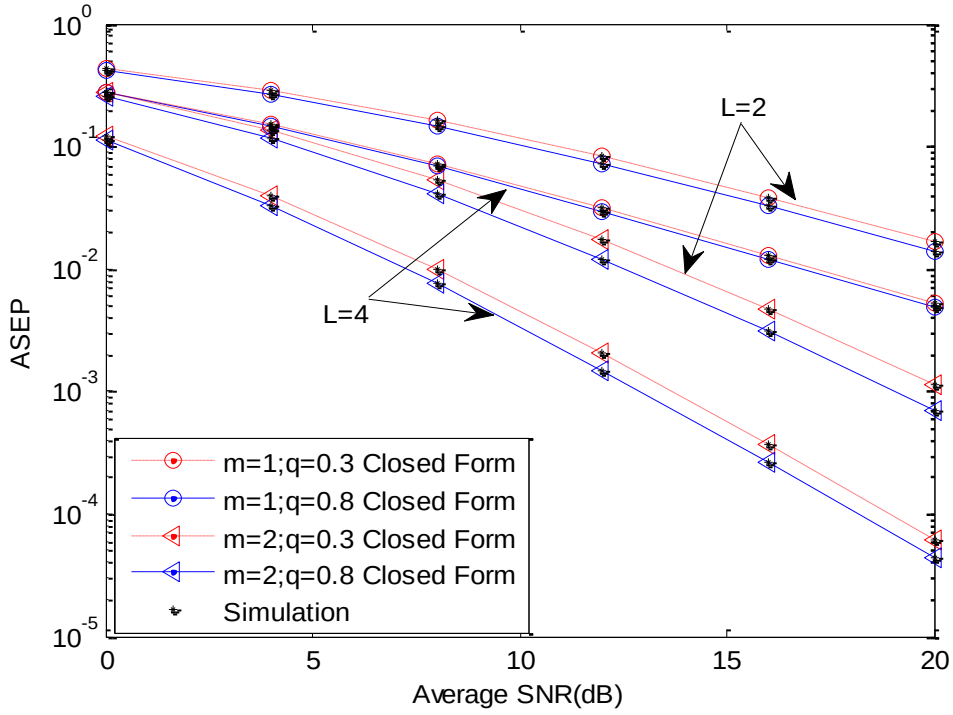

Figure 3.6 ASEP of DEQPSK for several values of m, q and L

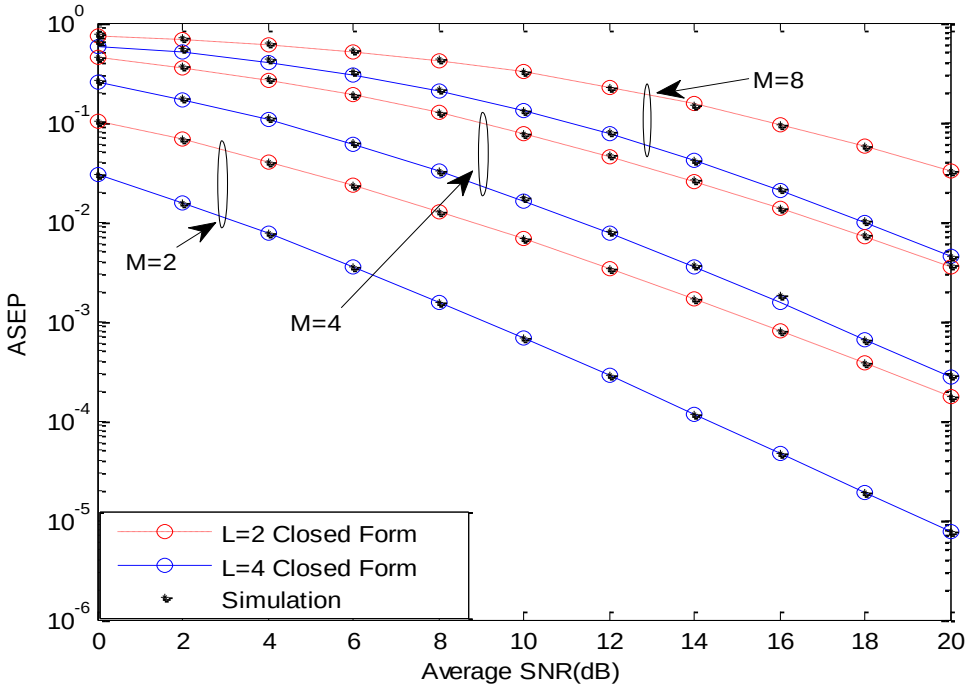

Figure 3.7 ASEP of M-QAM for several values of m and L

Table 3.2 *Number of terms (N) required for accuracy at 7th place of the decimal digit in the numerical evaluation of (3.14), (3.18) and (3.21)*

Modulation	L=1		L=4	
	q=0.4	q=0.8	q=0.4	q=0.8
BPSK (3.14)	14	2	26	4
QPSK (3.14)	16	3	29	5
8-PSK (3.14)	20	4	35	6
2-PAM (3.14)	11	2	21	3
8-PAM (3.14)	22	4	39	6
2-QAM (3.14)	14	2	27	4
8-QAM (3.14)	21	4	37	6
DEQPSK(3.14)	17	3	31	5
BFSK (3.18)	15	3	29	5
DQPSK (3.21)	13	2	27	4

The Comparison of QPSK and DQPSK schemes for different values of L is shown in Figure 3.5. As observed, an excellent match between the analytical results produced by putting closed-form expression of equation 3.14 for QPSK and equation 3.21 for DQPSK with the simulations results is achieved. It is noted that the performance of the system improves with an increase in L as shown by downshifting of the plots. Secondly, QPSK outperforms DQPSK significantly. In Figure 3.6, ASEP of DEQPSK has been plotted over the composite fading channel for several values of m, q and L. The theoretical curves have been constructed based on expression equation 3.14. It is observed that the plots shift downwards with the increase in the fading and shape parameters indicating an improvement in the system performance. Figure 3.7 demonstrates the plots for M-QAM using the analytical expression as given in equation 3.14 over L-Hoyt/gamma composite fading channel under the various constellation sizes M=2, 4 and 8. It is noted from the results that the plot shifts upwards for the higher constellation. ABEP/ASEP expressions presented here are presented in terms of infinite series. We have truncated the series by

including the finite number of terms N ensuring to achieve accuracy at the seventh place of the decimal digit. In Table 3.2, we have calculated the number of terms required to achieve this accuracy in equations 3.14, 3.18 and 3.21 as a function of q and L with m=1. The number of terms needed to achieve the desired accuracy depends on q, L and the modulation technique being used. The value of N decreases with increase in q, indicates that more number of terms are required for more severe fading conditions. It can be noted that more number of terms are required for higher diversity order system.

3.4 Significant Findings

Taking note of the fact that Hoyt is known to capture the severe multipath fading and gamma distribution is most widely used to model shadowing, we have analyzed the performance of L-Hoyt/gamma composite channel. The closed-form expressions for PDF of instantaneous SNR, AF, outage probability, channel capacity and ASEP/ABEP of the composite channel were obtained in terms of generalized hypergeometric functions. Moreover, the effect of fading parameters and diversity order on the system performance is discussed. All the results produced here are accompanied by Monte Carlo simulations.

This chapter is based on the following work:

Sandeep Kumar, *Sanjay Kumar Soni, Priyanka Jain, "Micro-Diversity Analysis of Error Probability and Channel Capacity over Hoyt/gamma Fading", Radioengineering, 2017, 26(4), 1096-1103. DOI: 10.13164/re.2017.1096. (**SCI journal with Impact factor – 1.048**)* [**110**]

CHAPTER 4

PERFORMANCE ANALYSIS OF *L*-HOYT/LOGNORMAL COMPOSITE FADING CHANNEL

This chapter evaluates the performance of communication systems with MRC diversity combining schemes over Hoyt/lognormal composite fading channels. A mixture gamma distribution is employed to approximate the PDF of the composite fading channel. The equivalent parameters of mixture gamma distribution are calculated. Thereafter, analytic expressions of the outage probability, ABEP and the average channel capacity for MRC schemes are provided.

4.1 System and Channel Model

PDF of γ for conditional Hoyt fading channel at the output of *L* branch MRC receiver is defined in equation 3.1. Here, shadowing is modeled using lognormal distribution with PDF given by equation 1.6. The composite PDF of *L*-Hoyt/lognormal can be evaluated by substituting equation 1.6 and 3.1 into equation 3.2 as

$$p_\gamma(\gamma) = \int_0^\infty \left(\frac{1+q^2}{2qw}\right)^L \frac{\exp\left[-\left(\frac{\left(1+q^2\right)\gamma}{2q^2w}\right)\right]}{\Gamma(L)} \gamma^{(L-1)}\, {}_1F_1\left(\frac{L}{2}; L; \frac{\left(1-q^4\right)\gamma}{2q^2w}\right) \times \frac{1}{\sigma w\sqrt{2\pi}} \exp\left(-\frac{\left(\log_e w-\mu\right)^2}{2\sigma^2}\right) dw \quad (4.1)$$

By replacing ${}_1F_1(.;.;.)$ using equation (9.210.1) of [**24**] and taking the assumption for *s* and *t* as in equation 3.4, the above equation can be solved as

$$p_\gamma(\gamma) = \sum_{n=0}^{\infty} \frac{s^L t^n \gamma^{(L+n-1)} \left(\frac{L}{2}\right)_n}{\Gamma(L+n)n!} \int_0^{\infty} \frac{1}{\sigma w\sqrt{2\pi}} w^{-(L+n)} \exp\left(-\frac{s\gamma}{qw}\right) \exp\left(-\frac{(\log_e w-\mu)^2}{2\sigma^2}\right) dw \tag{4.2}$$

Using the change of variable, $z = (\log_e w - \mu)/\sqrt{2}\sigma$ and putting $h(z) = \exp\left[-\left\{(n+L)(\sqrt{2}\sigma z+\mu) + (s\gamma/q)\exp\left\{-(\sqrt{2}\sigma z+\mu)\right\}\right\}\right]$, equation 4.2 can be written as

$$p_\gamma(\gamma) = \frac{1}{\sqrt{\pi}} \sum_{n=0}^{\infty} \frac{s^L t^n \gamma^{(L+n-1)} \left(\frac{L}{2}\right)_n}{\Gamma(L+n)n!} \int_{-\infty}^{+\infty} \exp(-z^2) h(z)\, dz \tag{4.3}$$

The term $\int_{-\infty}^{+\infty} \exp(-z^2) h(z)\, dz$ in equation 4.3 can be approximated as $\sum_{k=1}^{K} w_k h(z_k)$ using Gaussian-Hermite integration, where z_k and w_k are abscissas and weight factors. The values of z_k and w_k can be calculated by a simple MATLAB program. Therefore, the above equation can be simplified as

$$p_\gamma(\gamma) = \frac{C}{\sqrt{\pi}} \sum_{n=0}^{\infty} \frac{s^L t^n \gamma^{(L+n-1)} \left(\frac{L}{2}\right)_n}{\Gamma(L+n)n!} \sum_{k=1}^{K} w_k h(z_k) \tag{4.4}$$

where $C=\sqrt{\pi}\Big/\sum_{k=1}^{K}w_k$ is the normalized factor to ensure $\int_0^{\infty} p_{\gamma}(\gamma)d\gamma=1$. Doing some mathematical manipulations, equation 4.4 can be further simplified to

$$p_{\gamma}(\gamma)=\frac{s^L}{W}\sum_{n=0}^{\infty}\frac{t^n\gamma^{(L+n-1)}\left(\frac{L}{2}\right)_n}{\Gamma(L+n)n!}\sum_{k=1}^{K}w_k a_k\exp(-b_k\gamma) \tag{4.5}$$

The above distribution is a mixture of gamma distribution where $a_k=\exp\left\{-(n+L)\left(\sqrt{2\sigma^2 z_k}+\mu\right)\right\}$, $b_k=(s/q)\exp\left\{-\left(\sqrt{2\sigma^2 z_k}+\mu\right)\right\}$ and $W=\sum_{k=1}^{K}w_k$.

4.1.1 Outage Probability

Putting equation 4.5 in 1.13, the expression for outage probability is given as

$$P_{out}(\gamma_{th})=\frac{s^L}{W}\sum_{n=0}^{\infty}\frac{t^n\left(\frac{L}{2}\right)_n}{\Gamma(L+n)n!}\sum_{k=1}^{K}w_k\frac{a_k}{b_k^{(n+L)}}Y(n+L,\gamma_{th}) \tag{4.6}$$

4.1.2 Amount of Fading

The i^{th} moment of *L*-Hoyt/lognormal can be evaluated by putting equation 4.5 in the definition of i^{th} moment and using equation (07.34.03.0228.01) of [**107**], we get

$$E\left[\gamma^i\right]=\frac{s^L}{W}\sum_{n=0}^{\infty}\frac{t^n\left(\frac{L}{2}\right)_n}{\Gamma(L+n)n!}\sum_{k=1}^{K}w_k a_k\int_0^{\infty}\gamma^{(n+L+i)-1}G_{0,1}^{1,0}\left[b_k\gamma\Big|_0\right]d\gamma \tag{4.7}$$

Using equation (07.34.21.0009.01) of [**107**], equation 4.7 can be simplified as

$$E\left[\gamma^{i}\right]=\frac{s^{L}}{W}\sum_{n=0}^{\infty}\frac{t^{n}\left(\frac{L}{2}\right)_{n}}{\Gamma\left(L+n\right)n!}\sum_{k=1}^{K}w_{k}a_{k}\frac{\Gamma\left(n+L+i\right)}{b_{k}^{\left(n+L+i\right)}} \tag{4.8}$$

The final expression of AF can be easily evaluated by putting equation 4.8 in the AF expression.

4.1.3 Channel Capacity

Different adaptive transmissions schemes such as ORA, CIFR and TIFR are discussed in this section.

4.1.3.1 ORA

Channel capacity with ORA can be calculated by putting equation 4.5 in 3.8 and using equations (07.34.03.0228.01) and (07.03.0456.01) of [**107**], it can be written as

$$\begin{aligned}\frac{C_{ora}}{B}=&\frac{s^{L}}{\log_{10}\left(2\right)W}\sum_{n=0}^{\infty}\frac{t^{n}\left(\frac{L}{2}\right)_{n}}{\Gamma\left(L+n\right)n!}\sum_{k=1}^{K}w_{k}a_{k}\\&\times\int_{0}^{\infty}\gamma^{\left(n+L\right)-1}G_{2,2}^{1,2}\left[\gamma\middle|\begin{matrix}1,1\\1,0\end{matrix}\right]G_{0,1}^{1,0}\left[b_{k}\gamma\middle|_{0}\right]d\gamma\end{aligned} \tag{4.9}$$

Applying equation (07.34.21.0011.01) of [**107**], and doing some mathematical manipulation ORA channel capacity is evaluated as

$$\frac{C_{ora}}{B}=\frac{s^{L}}{\log_{10}\left(2\right)W}\sum_{n=0}^{\infty}\frac{t^{n}\left(\frac{L}{2}\right)_{n}}{\Gamma\left(L+n\right)n!}\sum_{k=1}^{K}w_{k}a_{k}G_{2,3}^{3,1}\left[b_{k}\middle|\begin{matrix}-\left(n+L\right),-\left(n+L-1\right)\\0,-\left(n+L\right),-\left(n+L\right)\end{matrix}\right] \tag{4.10}$$

4.1.3.2 CIFR

In this channel transmission policy, CSI is present at the transmitter. Using the result of equation 4.8 for $E\left[1/\gamma\right]$ in equation 3.10, one can easily find out the final expression of C_{cifr}.

4.1.3.3 TIFR

An improvement over CIFR is the TIFR, where the transmission is barred when the SNR falls below a fixed cut-off, γ_0 and to continue transmission when SNR is greater than γ_0. The outage capacity associated with a given P_{out} and corresponding cut-off is defined as [**1**]

$$C_{out} = B\log_2\left(1+\frac{1}{H}\right)\left(1-P_{out}\right) \tag{4.11}$$

P_{out} is defined in equation 4.6 and $H = \int_{\gamma_0}^{\infty} p_\gamma(\gamma)/\gamma d\gamma$. Using equation 4.5 and equation (3.381.3) of [**24**], *H* can be simplified as

$$H = \frac{s^L}{W}\sum_{n=0}^{\infty}\frac{t^n\left(\frac{L}{2}\right)_n}{\Gamma\left(L+n\right)n!}\sum_{k=1}^{K} w_k a_k \frac{\Gamma\left(L+n-1,\gamma_0 b_k\right)}{b_k{}^{(n+L-1)}} \tag{4.12}$$

TIFR capacity is obtained by maximizing the outage capacity for all possible γ_0, *i.e.* $C_{tifr} = \max_{\gamma_0} C_{out}$.

4.1.4 ASEP/ABEP

The general formula for ASEP/ABEP is given in equation 1.15. ASEP/ABEP for coherent and non-coherent modulation shall be examined separately in this section.

4.1.4.1 Coherent Modulation Scheme

In generic form, $P_e(\gamma)$ for coherent modulation scheme is given in equation 3.11. Putting equations 4.5 and 3.11 into equation 1.15, we get

$$\begin{aligned}\bar{P}_e \approx \frac{s^L}{W}\sum_{n=0}^{\infty}\frac{t^n\left(\frac{L}{2}\right)_n}{\Gamma(L+n)n!}\sum_{k=1}^{K}w_k a_k\sum_{d=1}^{D}\alpha_d \\ \times\int_0^{\infty}\gamma^{(n+L)-1}\exp(-b_k\gamma)\left(\frac{a_1}{2}\exp\left(-\frac{b_1c_0\gamma}{2}\right)+\frac{a_2}{2}\exp\left(-b_1c_0\gamma\right)\right)^d d\gamma\end{aligned} \tag{4.13}$$

α_d, c_0 and D have their usual meaning as given in Table 3.1. The value of the parameters a_1, a_2 and b_1 are same as defined in equation 3.12. This integral can be solved by using the same approach as used in solving the equation 3.13. Using equations (07.34.03.0228.01) and (07.34.21.0009.01) of [**107**], the generalized solution of ASEP for all formats of coherent modulation techniques is given by

$$\begin{aligned}\bar{P}_e \approx \frac{s^L}{W}\sum_{n=0}^{\infty}\frac{t^n\left(\frac{L}{2}\right)_n}{\Gamma(L+n)n!}\sum_{k=1}^{K}w_k a_k\sum_{d=1}^{D}\alpha_d \\ \times\sum_{r=0}^{d}C(d,r)\left(\frac{a_1}{2}\right)^{d-r}\left(\frac{a_2}{2}\right)^{r}\frac{\Gamma(L+n)}{\left[b_k+\frac{(d+r)b_1c_0}{2}\right]^{(L+n)}}\end{aligned} \tag{4.14}$$

4.1.4.2 Non-Coherent Modulation Scheme

In this section, we propose closed-form mathematical expression for non-coherent detection schemes over composite *L*-Hoyt/lognormal fading.

a) MFSK: The instantaneous bit error probability of MFSK is given in equation 3.17. The ABEP is obtained by substituting equation 4.5 and 3.17 into equation 1.15 and using equation (07.34.03.0228.01) of [**107**]

$$\bar{P}_e = \frac{s^L}{W}\sum_{n=0}^{\infty}\frac{t^n\left(\frac{L}{2}\right)_n}{\Gamma(L+n)n!}\sum_{k=1}^{K}w_k a_k \times\sum_{d=1}^{D}\alpha_d\sum_{m=1}^{M-1}C(M-1,m)\frac{(-1)^{m+1}}{m+1}\int_0^{\infty}\gamma^{(n+L)-1}G_{0,1}^{1,0}\left[\left[b_k+\frac{m}{(m+1)}\right]\gamma\middle|0\right]d\gamma \tag{4.15}$$

After using equation (07.34.21.0009.01) of [**107**], one can obtain the final expression of ABEP of MFSK as

$$\bar{P}_e = \frac{s^L}{W}\sum_{n=0}^{\infty}\frac{t^n\left(\frac{L}{2}\right)_n}{\Gamma(L+n)n!}\sum_{k=1}^{K}w_k a_k \times\sum_{d=1}^{D}\alpha_d\sum_{m=1}^{M-1}C(M-1,m)\frac{(-1)^{m+1}}{m+1}\frac{\Gamma(L+n)}{\left[b_k+\frac{m}{(m+1)}\right]^{(L+n)}} \tag{4.16}$$

b) DQPSK: Instantaneous bit error probability for DQPSK is defined in equation 3.19. Substituting equations 4.5 and 3.19 into equation 1.15 and using the expansion of Marcum-Q function and modified Bessel function [**13**], one can write the resulting expression using equation (07.34.03.0228.01) of [**107**] as

$$\bar{P}_e = \frac{s^L}{W}\sum_{n=0}^{\infty}\frac{t^n\left(\frac{L}{2}\right)_n}{\Gamma(L+n)n!}\sum_{k=1}^{K}w_k a_k \int_0^{\infty}\gamma^{(n+L)-1}G_{0,1}^{1,0}\left[\left[b_k+\frac{\left(a^2+b^2\right)}{2}\right]\gamma\middle|0\right] \times\left\{\sum_{v=0}^{\infty}\left(\frac{a}{b}\right)^v\sum_{u=0}^{\infty}\frac{\left(\frac{ab}{2}\gamma\right)^{2u+v}}{u!\Gamma(u+v+1)}-\frac{1}{2}\sum_{h=0}^{\infty}\frac{\left(\frac{ab}{2}\gamma\right)^{2h}}{(h!)^2}\right\}d\gamma \tag{4.17}$$

Using equation (07.34.21.0009.01) of [**107**], we can simplify equation 4.17 as shown

$$\bar{P}_e = \frac{s^L}{W}\sum_{n=0}^{\infty}\frac{t^n\left(\frac{L}{2}\right)_n}{\Gamma(L+n)n!}\sum_{k=1}^{K}w_k a_k \times\left\{\begin{array}{l}\displaystyle\sum_{v=0}^{\infty}\left(\frac{a}{b}\right)^v\sum_{u=0}^{\infty}\frac{\left(\frac{ab}{2}\right)^{2u+v}}{u!\Gamma(u+v+1)}\frac{\Gamma(L+n+2u+v)}{\left[b_k+\frac{\left(a^2+b^2\right)}{2}\right]^{(L+n+2u+v)}} \\ \displaystyle-\frac{1}{2}\sum_{h=0}^{\infty}\frac{\left(\frac{ab}{2}\right)^{2h}}{(h!)^2}\frac{\Gamma(L+n+2h)}{\left[b_k+\frac{\left(a^2+b^2\right)}{2}\right]^{(L+n+2h)}}\end{array}\right\} \tag{4.18}$$

4.2 Asymptotic Analysis

Asymptotic analysis is required where the channel is severely faded and large SNR is required for achieving a minimum target bit error rate. In this section, we have obtained asymptotic expressions for the ASEP/ABEP of the modulation technique produced in the earlier section. The asymptotic expressions can be derived based on the behavior of the

PDF of the instantaneous SNR around the origin [**111**]. By using Taylor,s series the PDF expression of equation 4.5 can be given as

$$p_{\gamma}(\gamma) = \frac{s^{L}}{W} \sum_{n=0}^{\infty} \frac{t^{n} \gamma^{(L+n-1)} \left(\frac{L}{2}\right)_{n}}{\Gamma(L+n) n!} \sum_{k=1}^{K} w_{k} a_{k} + O \tag{4.19}$$

where O is higher order terms and we can ignore them in our analysis.

4.2.1 Coherent Modulation Scheme

Putting equations 4.19 and 3.11 into equation 1.15, restoring to Binomial expansion and using equation (3.381.4) of [**24**], we get the final expression of ASEP is simplified as

$$\begin{aligned} \bar{P}_{e} \approx & \frac{s^{L}}{W} \sum_{n=0}^{\infty} \frac{t^{n} \left(\frac{L}{2}\right)_{n}}{\Gamma(L+n) n!} \sum_{k=1}^{K} w_{k} a_{k} \sum_{d=1}^{D} \alpha_{d} \\ & \times \sum_{r=0}^{d} C(d,r) \left(\frac{a_{1}}{2}\right)^{d-r} \left(\frac{a_{2}}{2}\right)^{r} \frac{\Gamma(L+n)}{\left[\frac{(d+r) b_{1} c_{0}}{2}\right]^{(L+n)}} \end{aligned} \tag{4.20}$$

4.2.2 Non-Coherent Modulation Scheme

a) MFSK

Putting equations 4.19 and 3.17 into equation 1.15, using equation (3.381.4) of [**24**] and after simplification, the asymptotic expression of ABEP of MFSK is given as

$$\bar{P}_e = \frac{s^L}{W}\sum_{n=0}^{\infty}\frac{t^n\left(\frac{L}{2}\right)_n}{\Gamma(L+n)n!}\sum_{k=1}^{K}w_k a_k \times\sum_{d=1}^{D}\alpha_d\sum_{m=1}^{M-1}C(M-1,m)\frac{(-1)^{m+1}}{m+1}\frac{\Gamma(L+n)}{\left[\frac{m}{(m+1)}\right]^{(L+n)}} \tag{4.21}$$

b) DQPSK

Putting equations 4.19 and 3.19 into equation 1.15 and using equation (3.381.4) of [**24**], we get the asymptotic expression of ABEP of DQPSK

$$\bar{P}_e = \frac{s^L}{W}\sum_{n=0}^{\infty}\frac{t^n\left(\frac{L}{2}\right)_n}{\Gamma(L+n)n!}\sum_{k=1}^{K}w_k a_k \times\left\{\begin{array}{l}\sum_{v=0}^{\infty}\left(\frac{a}{b}\right)^v\sum_{u=0}^{\infty}\frac{\left(\frac{ab}{2}\right)^{2u+v}}{u!\Gamma(u+v+1)}\frac{\Gamma(L+n+2u+v)}{\left[\frac{(a^2+b^2)}{2}\right]^{(L+n+2u+v)}} \\ -\frac{1}{2}\sum_{h=0}^{\infty}\frac{\left(\frac{ab}{2}\right)^{2h}}{(h!)^2}\frac{\Gamma(L+n+2h)}{\left[\frac{(a^2+b^2)}{2}\right]^{(L+n+2h)}}\end{array}\right\} \tag{4.22}$$

All the results produced for asymptotic analysis are in simplified form and can be directly used in the applications where higher SNR analysis is required.

4.3 Numerical Results and Discussions

In this section, numerical results are presented to illustrate the performance of composite *L*-Hoyt/lognormal channel. For all the calculations the values of *K* is taken as 4. The simulation results are in close match with the derived results obtained by keeping enough number of terms (*N*) in the infinite series. Outage probability vs. normalized outage threshold (γ/γ_{th}) based on equation 4.6 is shown in Figure 4.1. It is clear from the graph that system performance improves for the increase in diversity order. Indeed, as fading becomes less severe, the probability that the channel is in deep fade decreases significantly.

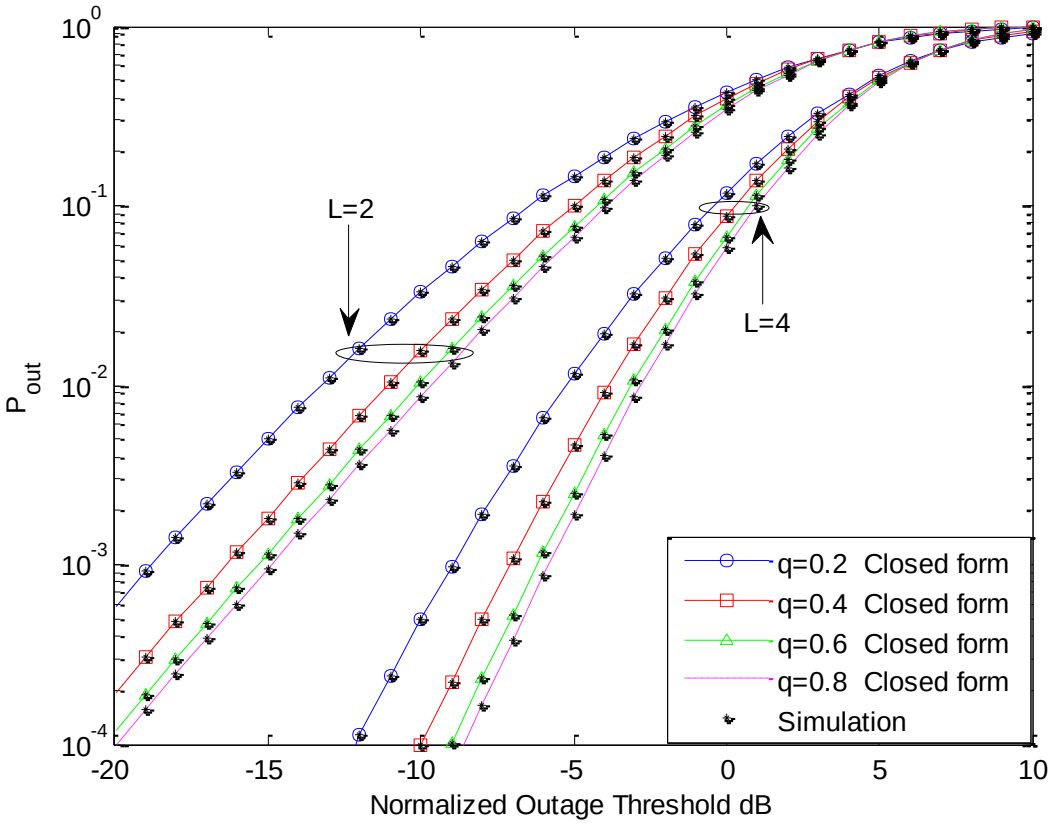

Figure 4.1 Outage probability vs. (γ/γ_{th}) ***for several values of q and L***

In Figure 4.2, the outage probability vs. (γ/γ_{th}). It is noted that the outage probability deteriorates as shadowing becomes heavier. AF as a function of the number of diversity branches using the closed-form expression as given in equation 4.8 is depicted in Figure 4.3. AF increases for an increase in σ and decrease in q. It is noted that a significant improvement in the system performance is achieved between L=1 and L=4. ASEP vs. average SNR for M-QAM is shown in Figure 4.4. System performance increases with increase in L and decreases in σ. Figure 4.5 shows the ASEP against average SNR for DEQPSK. As expected, ASEP deteriorates as the fading severity parameter q decreases.

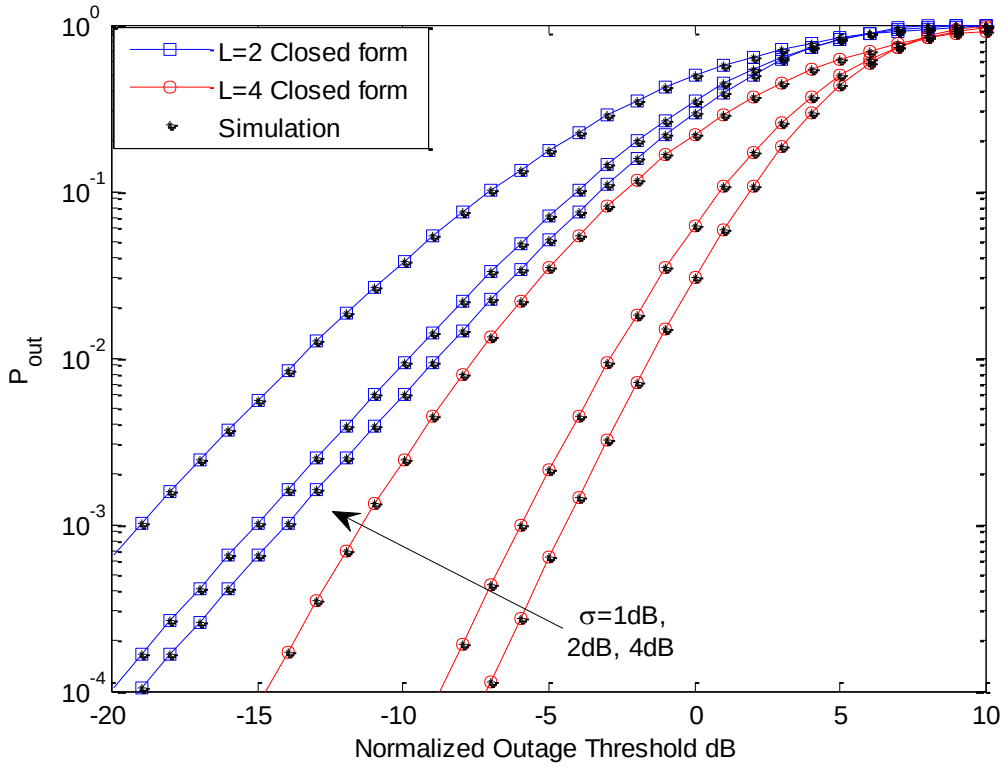

Figure 4.2 Outage probability vs. (γ/γ_{th}) ***with several values of σ and L***

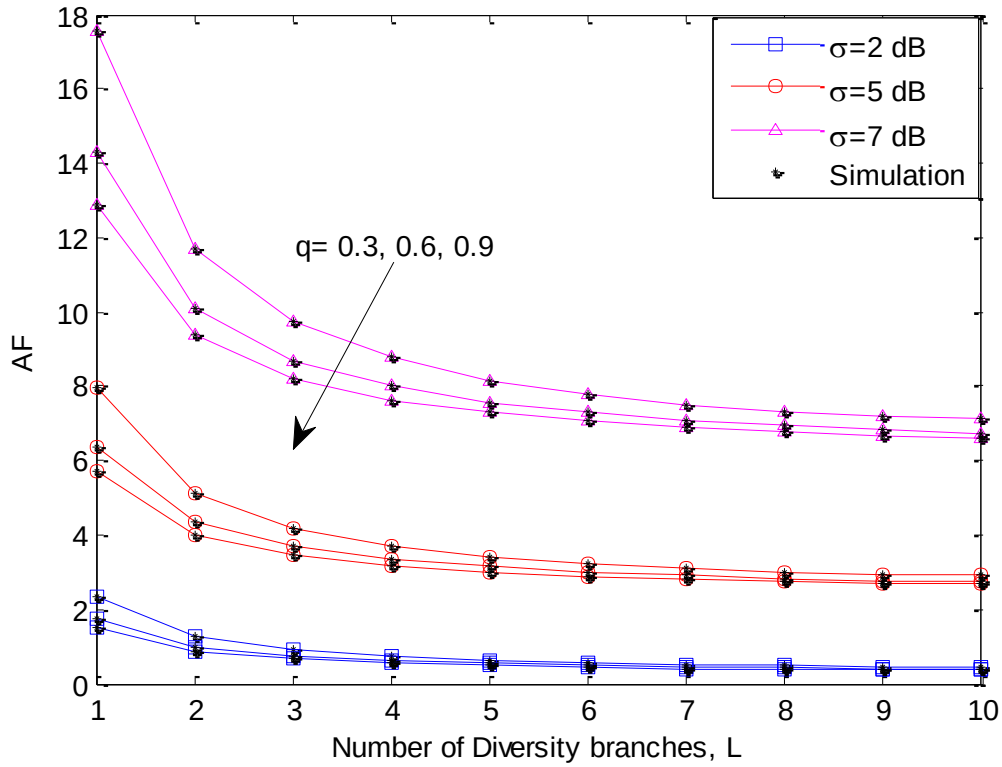

Figure 4.3 AF vs. L for different values of σ and q

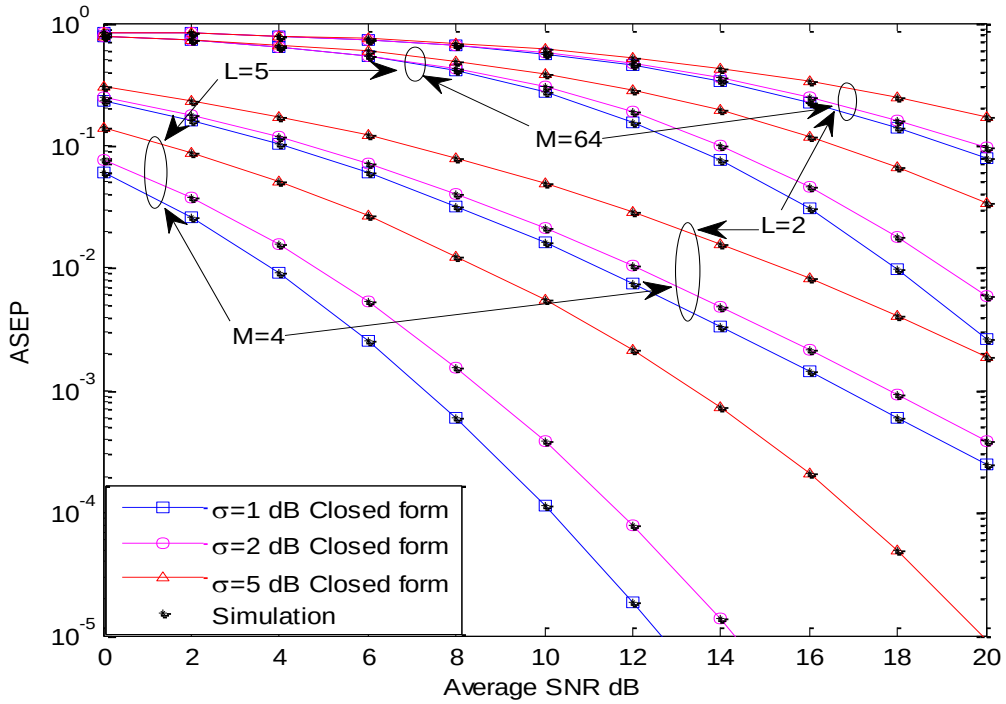

Figure 4.4 ASEP for coherent M-QAM for different values of σ and L

The theoretical curves in Figure 4.4 and 4.5 have been constructed based on equation 4.14. It is observed that the same behavior has been shown for P_{out} (Figure 4.1). In Figure 4.6, ABEP vs. average SNR for DQPSK is provided. It is very clear that the effect of the shadowing parameter is more pronounced compared to fading effect.

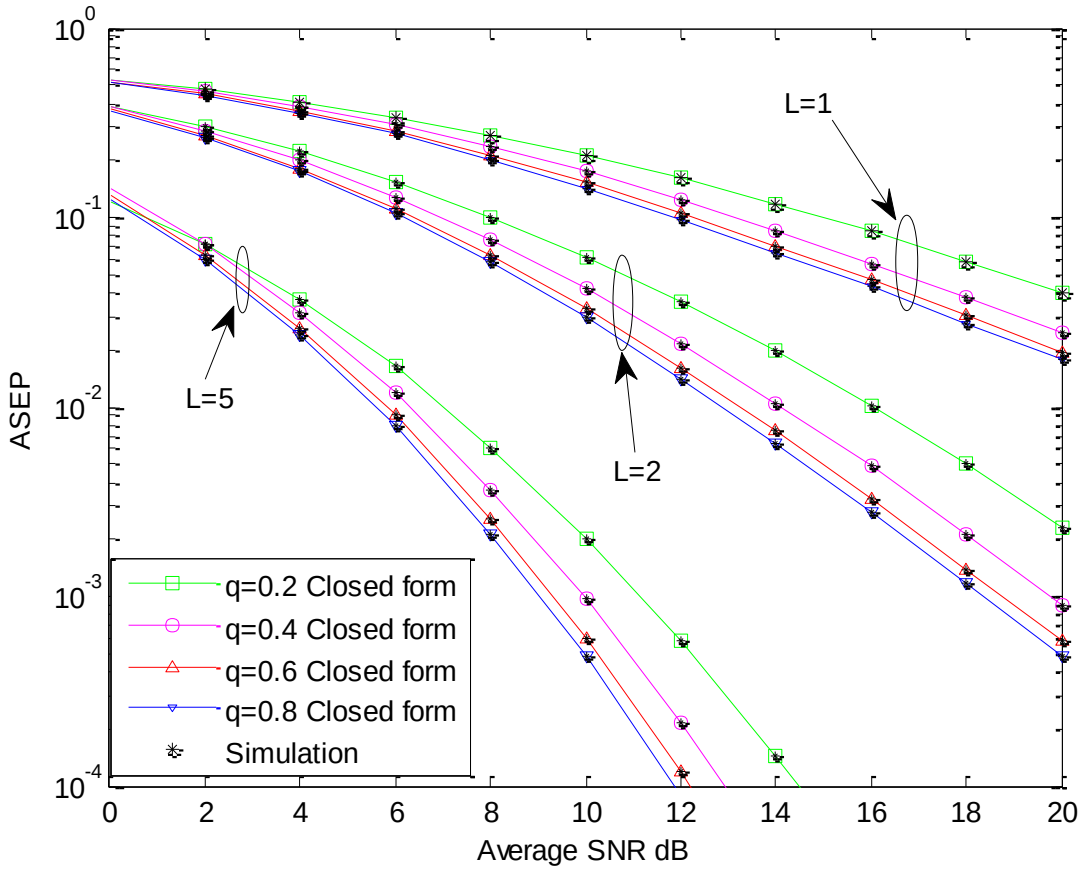

Figure 4.5 ASEP for coherent DEQPSK for different values of q and L

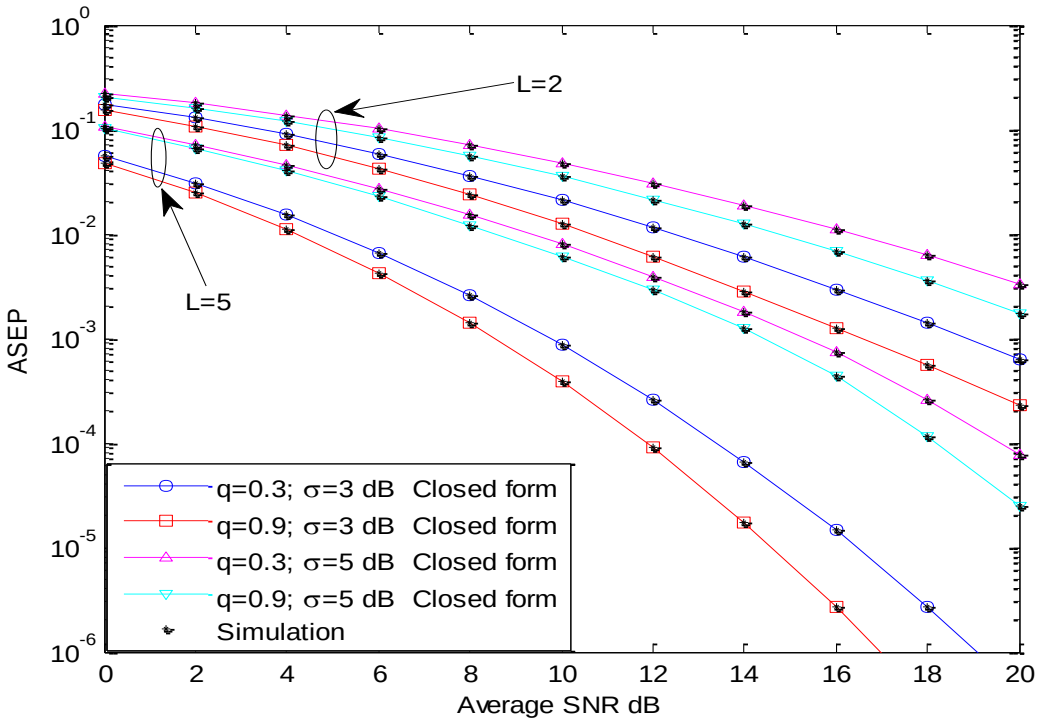

Figure 4.6 ASEP for non-coherent DQPSK for different values of σ, q and L

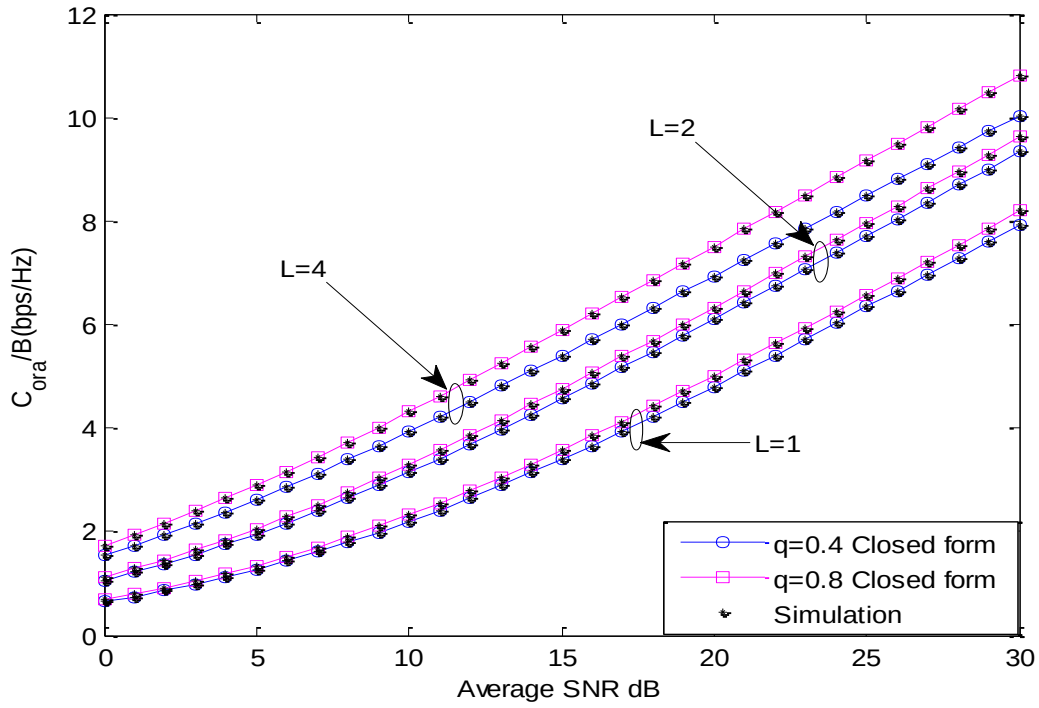

Figure 4.7 ORA channel capacity vs. average SNR for different values of q and L

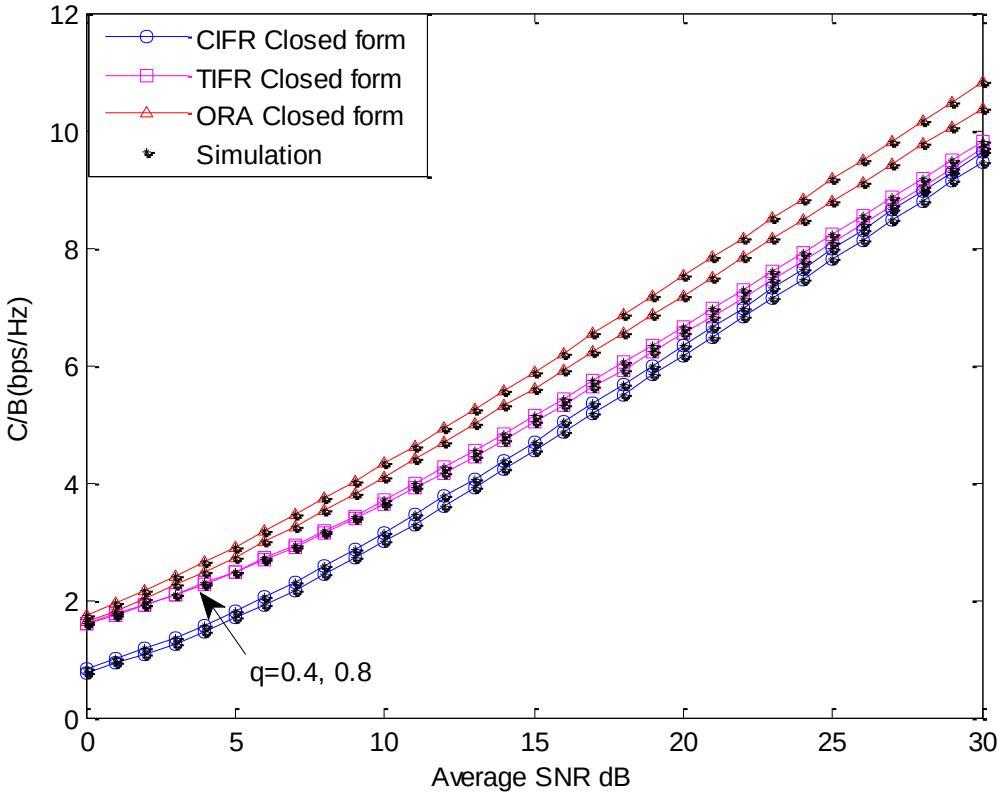

Figure 4.8 Average channel capacity as a function of the average SNR

In Figure 4.7, ORA channel capacity vs. average received SNR is plotted using the analytical expression given in equation 4.10. The results indicate that higher is the value of q and/or the higher is the value of L, higher is the channel capacity. It is observed that the performance difference between q=0.4 and q=0.8 plots increases for an increase in L. Figure 4.8 depicts the average channel capacity vs. average received SNR for the ORA, CIFR and TIFR schemes with L=4. It is noted that performance of TIFR is near to ORA in the low-power regime. The channel capacity of CIFR scheme is the lowest among all the channel capacities discussed here.

Table 4.1 *Number of terms (N) required for accuracy at 7th place of the decimal digit in the numerical evaluation of (4.14), (4.16) and (4.18) for various values of q and σ with L=2 and L=5*

Modulation	L=2						L=5					
	q=0.4			q=0.8			q=0.4			q=0.8		
	σ =5	σ =7	σ =10	σ =5	σ =7	σ =10	σ =5	σ =7	σ =10	σ =5	σ =7	σ =10
BPSK(4.14)	18	22	26	3	4	5	26	34	42	4	5	6
QPSK(4.14)	21	25	30	4	5	6	32	39	45	5	6	7
8-PSK(4.14)	27	30	34	5	6	7	39	43	48	6	7	8
2-PAM(4.14)	15	19	25	3	4	5	22	31	39	4	5	6
8-PAM(4.14)	29	32	35	5	6	7	44	47	49	6	7	8
2-QAM(4.14)	11	18	24	2	3	4	19	28	38	3	4	6
8-QAM(4.14)	28	31	35	5	6	7	40	44	49	6	7	8
DEQPSK(4.14)	22	26	31	4	5	6	33	41	47	5	6	7
BFSK(4.16)	19	23	26	4	5	6	27	36	44	5	6	7
DQPSK(4.18)	17	21	25	3	4	5	25	32	40	4	5	6

It is noted that by increasing the number of branches or at the higher value of *q*, the small value of the probability of error can be achieved. In the numerical evaluation of ASEP/ABEP expressions involving infinite series, we have truncated the series by including the finite number of terms (*N*) ensuring to achieve accuracy at the seventh place of the decimal digit. In Table 4.1, we have calculated the number of terms required to achieve this accuracy in equation 4.14, 4.16 and 4.18. The value of *N* decreases with increase in *q* indicates that more number of terms is required for more severe fading conditions. It is noted that more number of terms are required for higher diversity order system.

4.4 Significant Findings

In this chapter, we have derived the closed-form mathematical expression for *L*-Hoyt/lognormal composite fading channel using mixture gamma distribution. Performance parameters, such as P_{out}, AF, channel capacity and ASEP/ABEP for different modulation schemes, were expressed in closed form. All the results produced here are validated using Monte-Carlo/Exact simulations. The analytical results produced here can be useful in many wireless applications.

This chapter is based on the following work:

Sandeep Kumar, *Sanjay Kumar Soni, Priyanka, "Performance of MRC receiver over Hoyt/lognormal Composite Fading Channel", International Journal of Electronics, 2018, 105(9),1433-1450 DOI: https://doi.org/10.1080/00207217.2018.1460870,* ***(Taylor & Francis, Impact factor – 0.939)*** [**112**]

CHAPTER 5
PERFORMANCE ANALYSIS OF ENERGY DETECTOR OVER *L*-HOYT/GAMMA AND *L*-HOYT/LOGNORMAL FADING CHANNEL

This chapter studies the behavior of an energy detector over composite channels. The performance analysis of energy detector over *L*-Hoyt/gamma channel is studied in the first section followed by the performance evaluation over *L*-Hoyt/lognormal channel. The PDF approach is employed to derive the mathematical expressions of average probability of detection and the average area under the receiver operating characteristic over both the channels are derived. In addition, the optimized threshold has been evaluated to overcome the problem of SS at low SNR. Moreover, the performance of an energy detector is analyzed by deriving the average detection probability and the average AUC.

5.1 Energy Detector Performance over *L*-Hoyt/gamma

In this section, energy detection over *L*-Hoyt/gamma composite fading channel is performed.

5.1.1 Average Probability of Detection

In fading channel, $P_f(\lambda)$ in equation 1.21 will remain same, since it does not depends on the received SNR. But with the variation of channel gain, the probability of detection varies and hence it's averaging over SNR distribution needs to be evaluated.

Average probability of detection can be defined using equation 1.22 as

$$\overline{P_d}(\lambda)=\int_0^{\infty} P_d(\gamma,\lambda)p_\gamma(\gamma)d\gamma=\int_0^{\infty} Q_u\left(\sqrt{2\gamma},\sqrt{\lambda}\right)p_\gamma(\gamma)d\gamma \tag{5.1}$$

Substituting equations 3.5 and 1.24 into equation 5.1, $\overline{P_d}(\lambda)$ becomes

$$\begin{aligned}\overline{P_d}(\lambda)=\sum_{k=0}^{\infty}\sum_{n=0}^{\infty}&\frac{t^n\left(\frac{L}{2}\right)_n q^{n+L-m}}{\Gamma(L)\Gamma(m)(L)_n(n!)\overline{\gamma}^{m}s^{n-m}(k!)}\frac{\Gamma\left(u+k,\frac{\lambda}{2}\right)}{\Gamma(u+k)}\\&\times\int_0^{\infty}\gamma^{k+m-1}e^{-\gamma}G_{0\ 2}^{2\ 0}\left[\frac{s\gamma}{q\overline{\gamma}}\middle|_{0,\ (n+L-m)}\right]d\gamma\end{aligned} \tag{5.2}$$

Using equations (07.34.03.0228.01) and (07.34.21.0009.01) of [**107**], equation 5.2 can be simplify as

$$\begin{aligned}\overline{P_d}(\lambda)=\sum_{k=0}^{\infty}\sum_{n=0}^{\infty}&\frac{t^n\left(\frac{L}{2}\right)_n q^{n+L+k}\overline{\gamma}^{k}}{\Gamma(L)\Gamma(m)(L)_n(n!)s^{n+k}(k!)}\\&\times\frac{\Gamma\left(u+k,\frac{\lambda}{2}\right)}{\Gamma(u+k)}G_{2\ 1}^{1\ 2}\left[\frac{q\overline{\gamma}}{s}\middle|_{1-(k+m),\ 1-(n+L+k)}\right]\end{aligned} \tag{5.3}$$

Average probability of missed detection, $\overline{P}_m(\lambda)$ can easily be calculated by putting equation 5.3 in $\overline{P}_m(\lambda)=\left[1-\overline{P}_d(\lambda)\right]$.

5.1.2 Average Area under the ROC curve

AUC is another performance parameter that gives a better understanding of the performance of energy detector. It is difficult to compare the performance of two energy detectors based on visual perception of their ROC when their ROC curves cross each other. In that situation, AUC is the single figure of merit that provides a better understanding as to what factors it affects the performance of the energy detector. In [2], it was indicated that the average AUC shows the probability of adopting the appropriate decision. The value of AUC varies from 0.5 to 1 as the detection threshold varies from 0 to ∞ [**91**]. The average AUC ($\overline{A}$) can be defined by [**90**] as

$$\overline{A} = -\int_0^{\infty} \overline{P_d}(\lambda) \frac{\partial P_f(\lambda)}{\partial \lambda} d\lambda \tag{5.4}$$

where

$$\frac{\partial P_f(\lambda)}{\partial \lambda} = -\frac{\lambda^{u-1} e^{-\lambda/2}}{2^u \Gamma(u)} \tag{5.5}$$

Substituting equations 5.3 and 5.5 into equation 5.4, we have

$$\begin{aligned} \overline{A} = \sum_{k=0}^{\infty}\sum_{n=0}^{\infty} \frac{t^n \left(\frac{L}{2}\right)_n q^{n+L+k} \overline{\gamma}^k}{\Gamma(L)\Gamma(m)(L)_n (n!) s^{n+k} (k!)} G_{2\,1}^{1\,2}\left[\frac{q\overline{\gamma}}{s} \middle| \begin{matrix} 1-(k+m),\ 1-(n+L+k) \end{matrix} \right] \\ \times \frac{1}{2^u \Gamma(u)\Gamma(u+k)} \int_0^{\infty} \lambda^{u-1} e^{-\lambda/2} \Gamma\left(u+k, \frac{\lambda}{2}\right) d\lambda \end{aligned} \tag{5.6}$$

Using equations (07.34.03.0228.01) of [**107**] and equation (6.455.1) of [**24**] the closed-form mathematical expression of average AUC is given as

$$\overline{A}=\sum_{k=0}^{\infty}\sum_{n=0}^{\infty}\frac{t^{n}\left(\mathrm{L}/2\right)_{n}q^{n+L+k}\overline{\gamma}^{k}}{\Gamma\left(J\right)\Gamma\left(m\right)\left(J\right)_{n}\left(n!\right)s^{n+k}\left(k!\right)}\frac{1}{\Gamma\left(u+k\right)}G_{2\ 1}^{1\ 2}\left[\frac{q\overline{\gamma}}{s}\middle|_{1-(k+m),\ 1-(n+L+k)}\right] \times\frac{\Gamma\left(2u+k\right)}{2^{2u+k}\left(u!\right)\Gamma\left(u+k\right)}{}_{2}F_{1}\left(1,\ 2u+k;\ u+1;\ 1/2\right) \tag{5.7}$$

5.1.3 Threshold Optimization

The total probability of error can be expressed by [**112**] as

$$P_{e}=P\left(H_{0}\right)\overline{P}_{f}\left(\lambda\right)+P\left(H_{1}\right)\overline{P}_{m}\left(\lambda\right) \tag{5.8}$$

The optimum threshold can be obtained by differentiating equation 5.8 with respect to λ and to find a global minimum, as the second derivative of the total probability of error w.r.t threshold is the positive value. Hence, we can find the optimized value of λ as

$$\lambda_{opt}=arg\,min_{\lambda}\left(P_{e}\right) \tag{5.9}$$

Considering apriori probability of both the hypothesis to be same in equation 5.8, we have

$$\frac{\partial\overline{P_{f}}\left(\lambda\right)}{\partial\lambda}+\frac{\partial\overline{P_{m}}\left(\lambda\right)}{\partial\lambda}=0 \tag{5.10}$$

The first term of equation 5.10 is obtained in equation 5.5 and the second term $\partial\overline{P_{m}}\left(\lambda\right)/\partial\lambda=\partial\left(1-\overline{P_{d}}\left(\lambda\right)\right)/\partial\lambda=-\partial\overline{P_{d}}\left(\lambda\right)/\partial\lambda$ is obtained as

$$\frac{\partial \overline{P_d}(\lambda)}{\partial \lambda} = -\sum_{k=0}^{\infty}\sum_{n=0}^{\infty} \frac{t^n \left(\mathrm{L}/2\right)_n q^{n+L+k} \overline{\gamma}^k}{\Gamma(L)\Gamma(m)(L)_n (n!) s^{n+k} (k!)} \times G_{2\ 1}^{1\ 2}\left[\frac{q\overline{\gamma}}{s} \middle| \begin{matrix} 1-(k+m),\ 1-(n+L+k) \\ \end{matrix} \right] \frac{\lambda^{u+k-1} e^{-\lambda/2}}{2^{u+k}\Gamma(u+k)} \tag{5.11}$$

Substituting equations 5.5 and 5.11 into equation 5.10, we have

$$\sum_{k=0}^{\infty}\sum_{n=0}^{\infty} \frac{t^n \left(\mathrm{L}/2\right)_n q^{n+L+k} \overline{\gamma}^k}{\Gamma(L)\Gamma(m)(L)_n (n!) s^{n+k} (k!)} \frac{\lambda^k \Gamma(u)}{2^k \Gamma(u+k)} \times G_{2\ 1}^{1\ 2}\left[\frac{q\overline{\gamma}}{s} \middle| \begin{matrix} 1-(k+m),\ 1-(n+L+k) \\ \end{matrix} \right] = 1 \tag{5.12}$$

From equation 5.12, we can calculate the optimum value of threshold numerically.

5.2 Energy Detector Performance over L-Hoyt/Lognormal

In this section, energy detection over *L*-Hoyt/lognormal composite fading channel is performed.

5.2.1 Average Probability of Detection

For L-Hoyt/lognormal fading channel, the average probability of detection, $\overline{P}_d(\lambda)$ can be calculated by putting equations 4.5 and 1.24 into equation 5.1 and is given as

$$\bar{P}_d(\lambda) = \frac{s^L}{W}\sum_{g=0}^{\infty}\sum_{n=0}^{\infty}\frac{t^n\left(\frac{L}{2}\right)_n}{\Gamma(L+n)n!g!}\sum_{k=1}^{K}w_k a_k \times \frac{\Gamma\left(u+g,\lambda/2\right)}{\Gamma(u+g)}\int_0^{\infty}\gamma^{(n+L+g)-1}\exp\left\{-\gamma\left(1+b_k\right)\right\}d\gamma \tag{5.13}$$

Using equations (07.34.03.0228.01) and (07.34.21.0009.01) of [**107**], we can simplify equation 5.13 as

$$\bar{P}_d(\lambda) = \frac{s^L}{W}\sum_{g=0}^{\infty}\sum_{n=0}^{\infty}\frac{t^n\left(\frac{L}{2}\right)_n}{\Gamma(L+n)n!g!}\sum_{k=1}^{K}w_k a_k \times \frac{\Gamma\left(u+g,\lambda/2\right)}{\Gamma(u+g)}\frac{\Gamma(L+n+g)}{\left[1+b_k\right]^{(L+n+g)}} \tag{5.14}$$

Using the same approach as discussed above, $\bar{P}_d(\lambda)$ in terms of lower incomplete gamma function can also be written as

$$\bar{P}_d(\lambda) = \frac{s^L}{W}\sum_{n=0}^{\infty}\frac{t^n\left(\frac{L}{2}\right)_n}{\Gamma(L+n)n!}\sum_{k=1}^{K}w_k a_k \times\left\{\frac{\Gamma(L+n)}{\left[b_k\right]^{(L+n)}}-\sum_{g=0}^{\infty}\frac{Y\left(u+g,\lambda/2\right)}{g!\Gamma(u+g)}\frac{\Gamma(L+n+g)}{\left[1+b_k\right]^{(L+n+g)}}\right\} \tag{5.15}$$

5.2.2 Average Area under the ROC curve

The average AUC as given in equation 5.4 can be redefined by [**91**] as

$$\bar{A} = \frac{1}{2^u\Gamma(u)}\int_0^{\infty}\lambda^{u-1}\exp\left(-\frac{\lambda}{2}\right)\bar{P}_d(\lambda)\,d\lambda \tag{5.16}$$

Putting equation 5.15 in the above equation, using equation (3.381.4) of [**24**] and equation (2.10.3.2) of [**113**], the analytical expression of $\bar{A}$ can be obtained as

$$\bar{A} = \frac{s^L}{W}\sum_{n=0}^{\infty}\frac{t^n\left(\frac{L}{2}\right)_n}{\Gamma(L+n)n!}\sum_{k=1}^{K}w_k a_k \times\left\{\frac{\Gamma(L+n)}{[b_k]^{(L+n)}}-\sum_{g=0}^{\infty}\frac{\Gamma(L+n+g)}{\Gamma(u)g!\Gamma(u+g+1)}\frac{\Gamma(2u+g)}{[1+b_k]^{(L+n+g)}}\,{}_2F_1(u+g,2u+g;u+g+1;-1)\right\} \tag{5.17}$$

It is necessary to know the error in such truncation of the infinite series. An expression for the upper bound on the truncation error in equation 5.17 by *R* number of terms is given as

$$\begin{aligned} E_R \le \frac{s^L}{W}\sum_{n=0}^{\infty}\frac{t^n\left(\frac{L}{2}\right)_n}{\Gamma(L+n)n!}\sum_{k=1}^{K}w_k a_k \frac{1}{[1+b_k]^{(L+n+R)}}\frac{\Gamma(2u+R)\Gamma(L+n+R)}{\Gamma(u)\Gamma(R+1)\Gamma(u+R+1)} \\ \times\,{}_3F_2\left(1,L+n+R,2u+R;R+1,u+R+1;\frac{1}{1+b_k}\right) \\ \times\,{}_2F_1(u+R,2u+R;u+R+1;-1) \end{aligned} \tag{5.18}$$

Proof: See Appendix B.

5.2.3 Optimization of Detection Threshold

Deciding detection threshold parameter is crucial for accurate estimation of the available spectrum. The probability of error is expressed in equation 5.8. The optimum threshold can be obtained by using equation 5.9 and considering both the hypothesis equally

probable. By using the identity of differentiation of gamma function as used in 5.11, the final expression of detection threshold optimization can be derived as

$$\frac{s^L}{W}\sum_{g=0}^{\infty}\sum_{n=0}^{\infty}\frac{t^n\left(\frac{L}{2}\right)_n}{\Gamma(L+n)n!}\sum_{k=1}^{K}w_k a_k \frac{\Gamma(L+n+g)}{\left[1+b_k\right]^{(L+n+g)}}\frac{\lambda^g\Gamma(u)}{2^g\Gamma(u+g)}=1 \tag{5.19}$$

Solving equation 5.19 numerically, we get the optimum value of the threshold.

5.3 Numerical Results and Discussions

The energy detector performance over *L*-Hoyt/gamma and *L*-Hoyt/lognormal fading channel are demonstrated in this section.

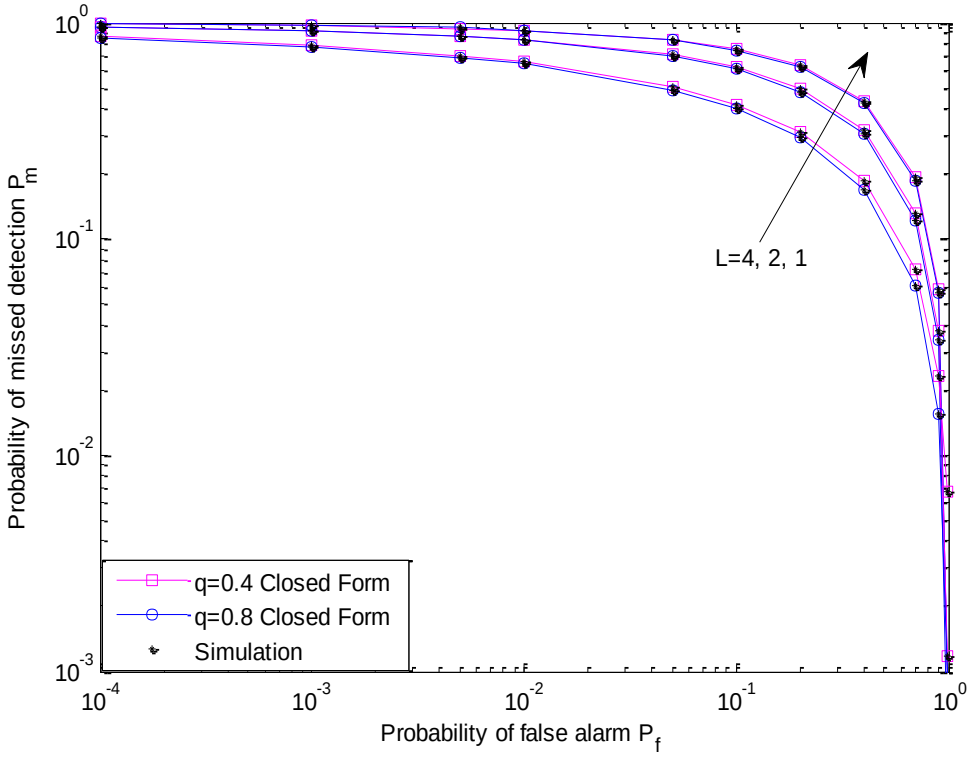

Figure 5.1 CROC curves with several values of fading parameters for L-Hoyt/gamma channel

The CROC curves for various values of fading parameter and diversity order with $u=8$ have been plotted in Figure 5.1 based on equation 5.3. When no diversity is applied, the probability of detection is low for q=0.4, 0.8 and the gap between the plots is very less, but as the diversity order increases the gap between the plots increases. It can be observed that there exists an obvious diversity gain when MRC is employed compared to the single antenna case. Moreover, as q increases, a higher detection probability with a lower false alarm probability is observed because the channel fading conditions improve, that is, the fluctuation of the signal strength reduces.

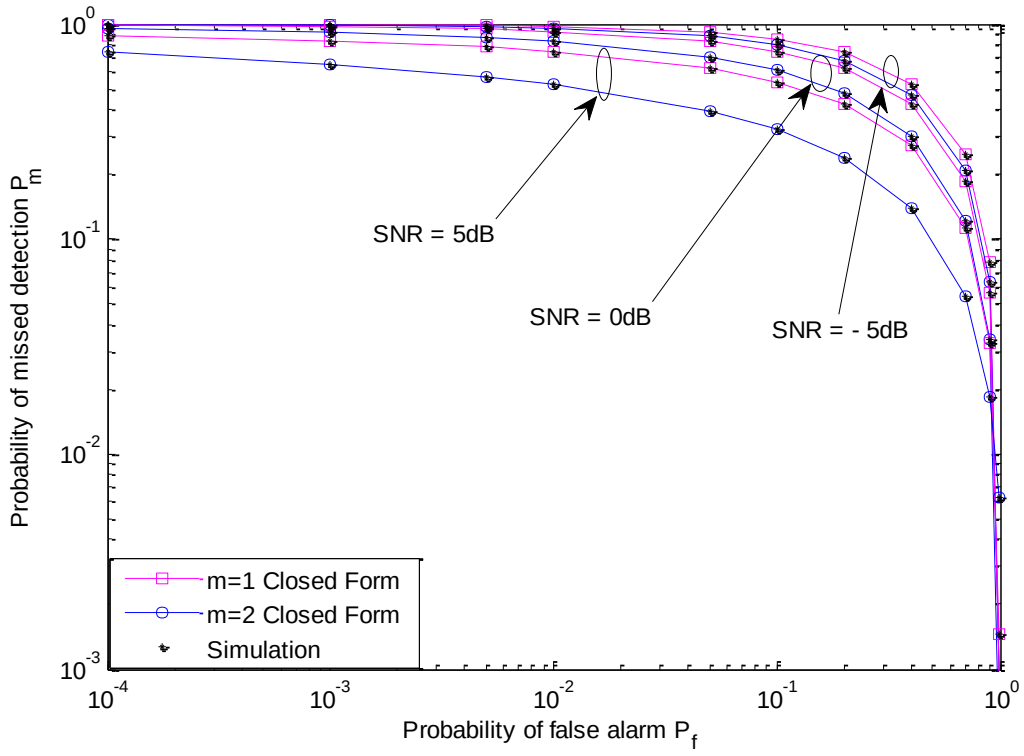

Figure 5.2 CROC curves with several values of gamma parameters for L-Hoyt/gamma channel

In Figure 5.2, CROC curves for different values of SNR and *m* are plotted. At SNR = -5 dB, CROC curves for $m = 1, 2$ are very close and the gap between the curves increases for the increase in SNR values. It shows that the probability of missed detection is high at low SNR but as the SNR increases, the probability of missed detection decreases. Though, for the small value of SNR, the output of energy detector is providing satisfactory performance, but as the SNR increases, energy detector based detection improved even when the gamma fading parameter increases.

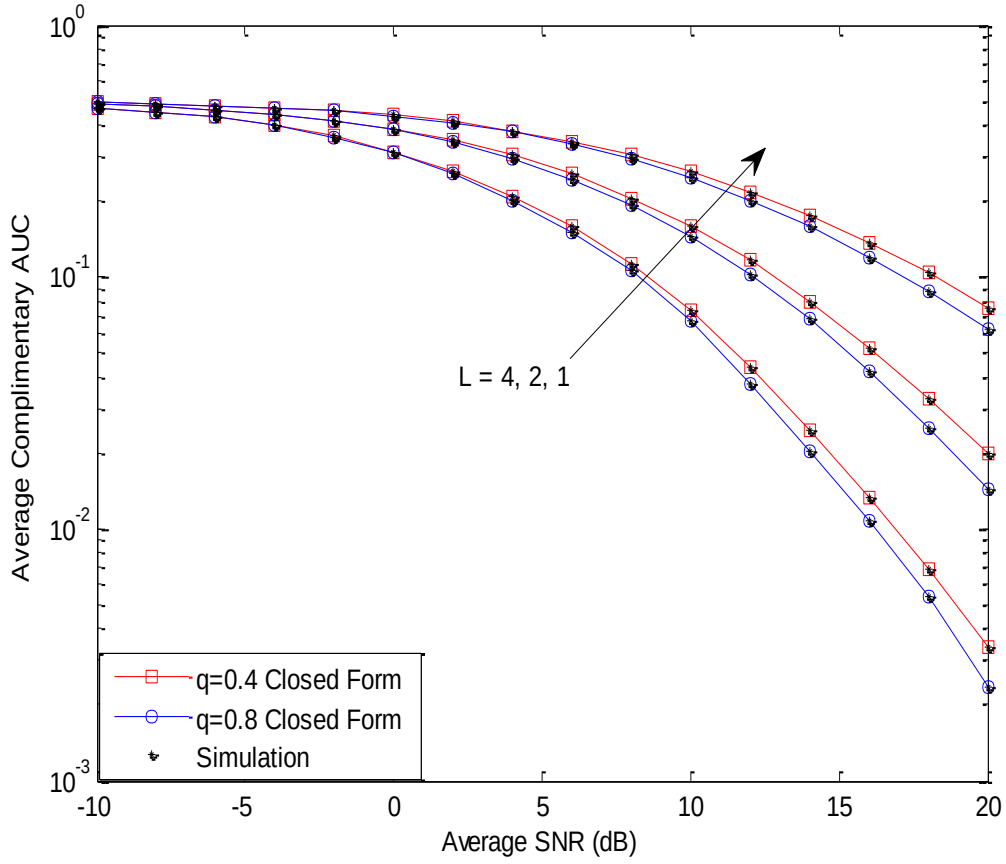

Figure 5.3 CAUC against the average received SNR with several values of fading parameters and diversity branches for L-Hoyt/lognormal channel

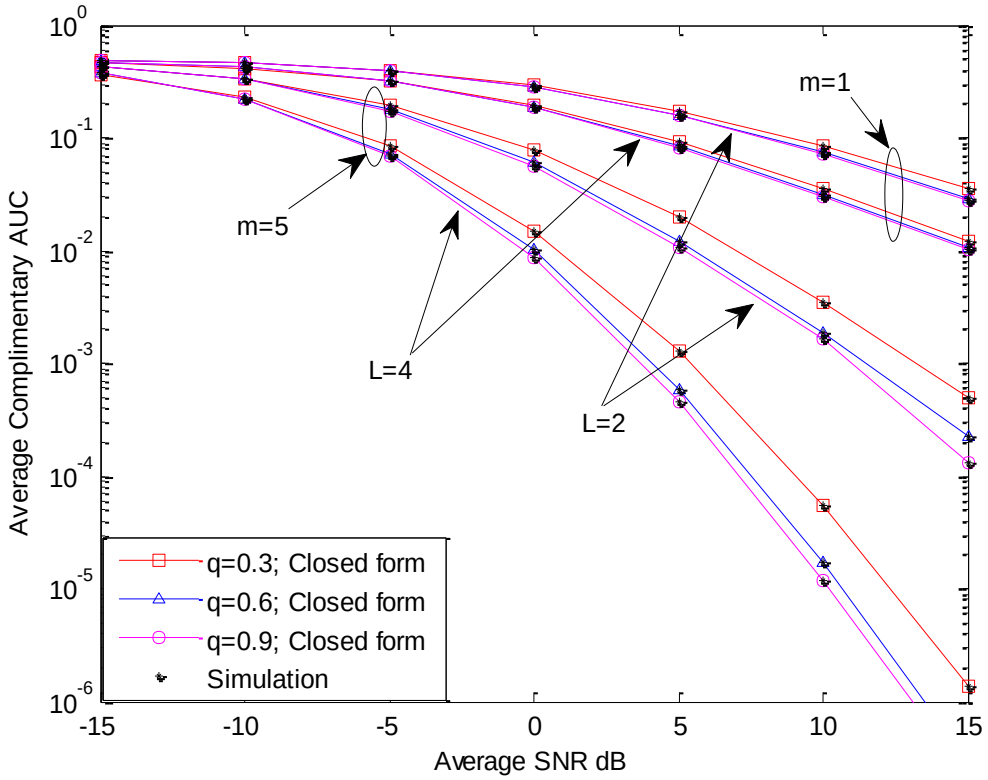

Figure 5.4 CAUC as a function average SNR with several values of m, q and L for L-Hoyt/gamma channel

In Figure 5.3, average CAUC curves for various values of diversity order and fading parameters are portrayed using the closed-form expression as given in equation 5.17. It is interesting to note that with the increase in the received SNR, the value of CAUC decreases indicating that the ROC plots shifted upward signifying an improvement in the detector performance. Also, it can be observed that the performance gap between q=0.4 and q=0.8 increases with higher SNR. It is very much clear that diversity reception can be potentially used to increase the detector's performances. As the average SNR increases, average CAUC curves decreases for both the values of fading parameters. For L=1, average CAUC curves decrease at a very high value of average SNR and at

$q = 0.4, 0.8$, the average CAUC curves are very close to each other, but as the diversity order increases, the performance of energy detector improves very significantly even at both the fading parameters as shown in the plot. The variation of CAUC, (1 - $\bar{A}$) as a function of $\bar{\gamma}$ is plotted in Figure 5.4. The effect of diversity can be observed from the plots. The theoretical curves have been constructed based on equation 5.7. It is clearly shown that the analytical results produced here match well with their Monte-Carlo simulation counterparts, verifying the accuracy of the mathematical expressions.

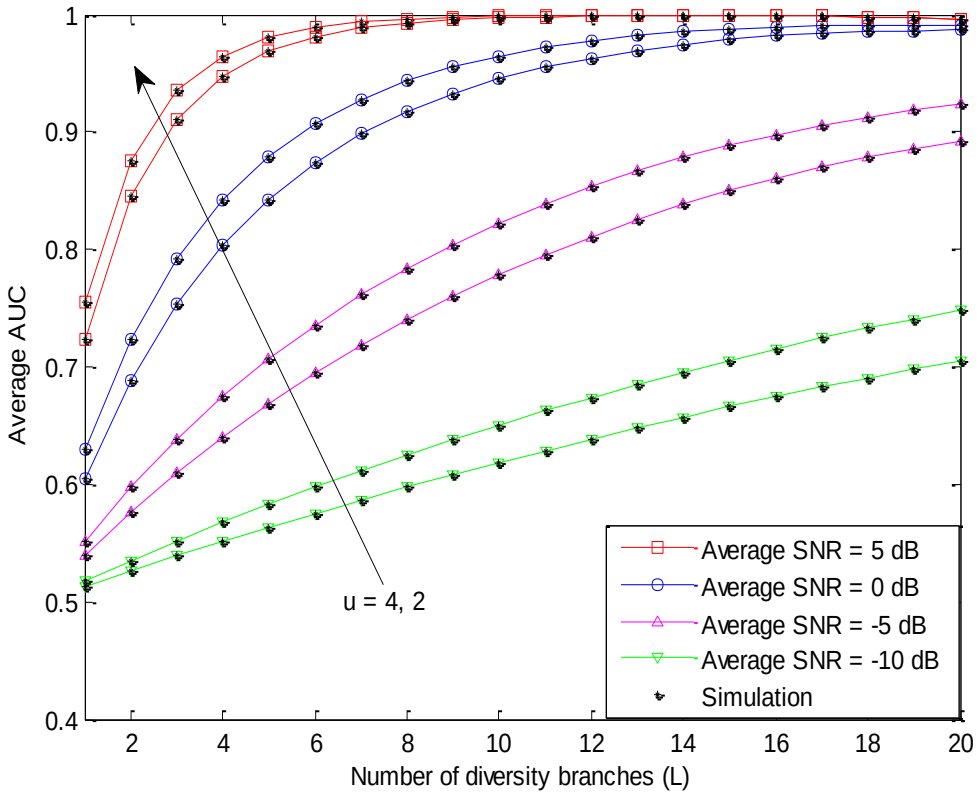

Figure 5.5 Average AUC against diversity branches for various values of average received SNR and number of samples

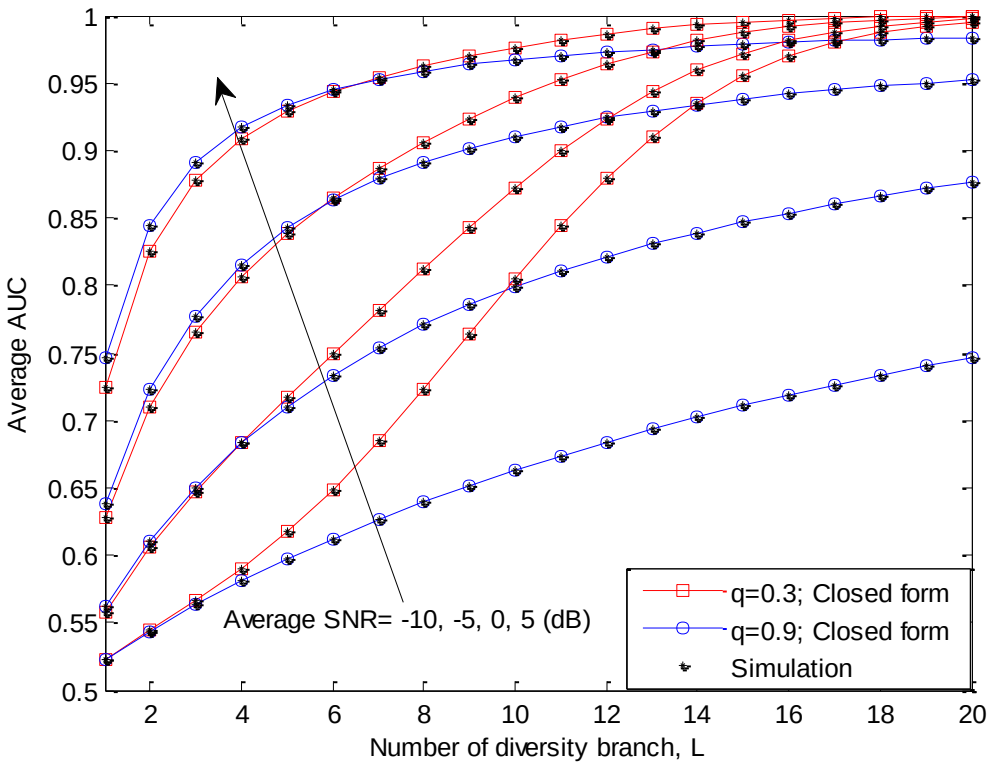

Figure 5.6 Average AUC against diversity order for various values of fading parameters and average received SNR

AUC against diversity branches for various values of the average received SNR and number of samples is shown in Figure 5.5. As SNR decreases, the average AUC curve shifts downwards but exactly opposite behavior is expressed for *u*. Hence, it is very much clear from the plot that as the number of diversity branches increases, the average AUC curve moves towards its optimum value, i.e., 1. At the low value of SNR i.e., -10 dB, average AUC curves are not converging towards unity for different values of *u*, but as the value of SNR increases towards higher values, 0 dB and 5 dB, the average AUC curves conversed towards unity. Hence, from the figure, it is very much clear that average AUC always lies between 0.5 and 1.

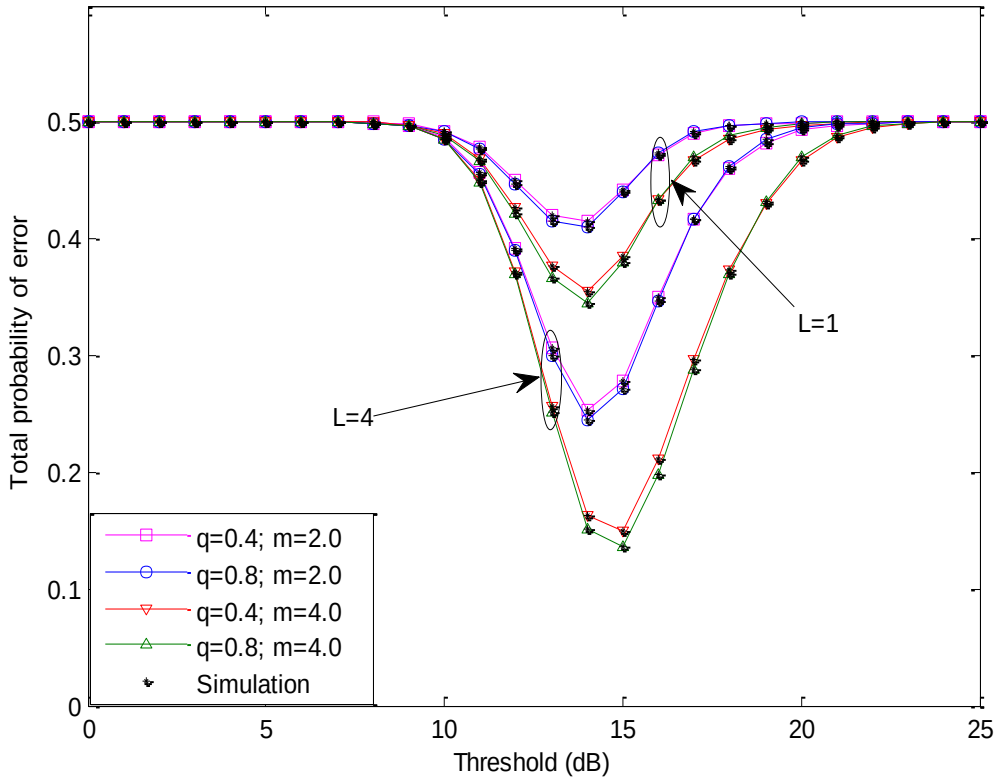

Figure 5.7 Probability of error as a function of threshold parameter with several values of fading parameters, gamma parameters and diversity branches for L-Hoyt/gamma channel

Average AUC curves against the number of diversity branches are shown in Figure 5.6. As average SNR decreases, average AUC curve shift downwards. Hence, it is very much clear from the plots that as the number of diversity branches increases, average AUC curve moves towards its optimum value i.e. 1. It is interesting to note that up to a certain order of diversity the system performance increases with increase in the value of fading parameter and afterward the behavior of fading parameter with system performance reverses. The threshold optimization has been considered in Figure 5.7 using the analytical expression as given in equation 5.8 over *L*-Hoyt/gamma composite fading channel. The inverted bell-shaped has been shown at different diversity order, different

fading parameters ($q=0.4,0.8$) and for different gamma parameter ($m=2,4$). It is observed that the total probability of error (P_e) has global minima with respect to the threshold (λ). The total probability of error decreases as the number of diversity order increases but when no diversity case is considered, not enough improvement has been seen in the plot. When we consider, at *L*=1 the probability of error are very close to each other for different values of *q* and *m=2*, but for different values of *m*, the total probability of error decreases even at single diversity order. So, when the diversity order increases form *L*=1 to *L*=4, the performance of energy detector improves.

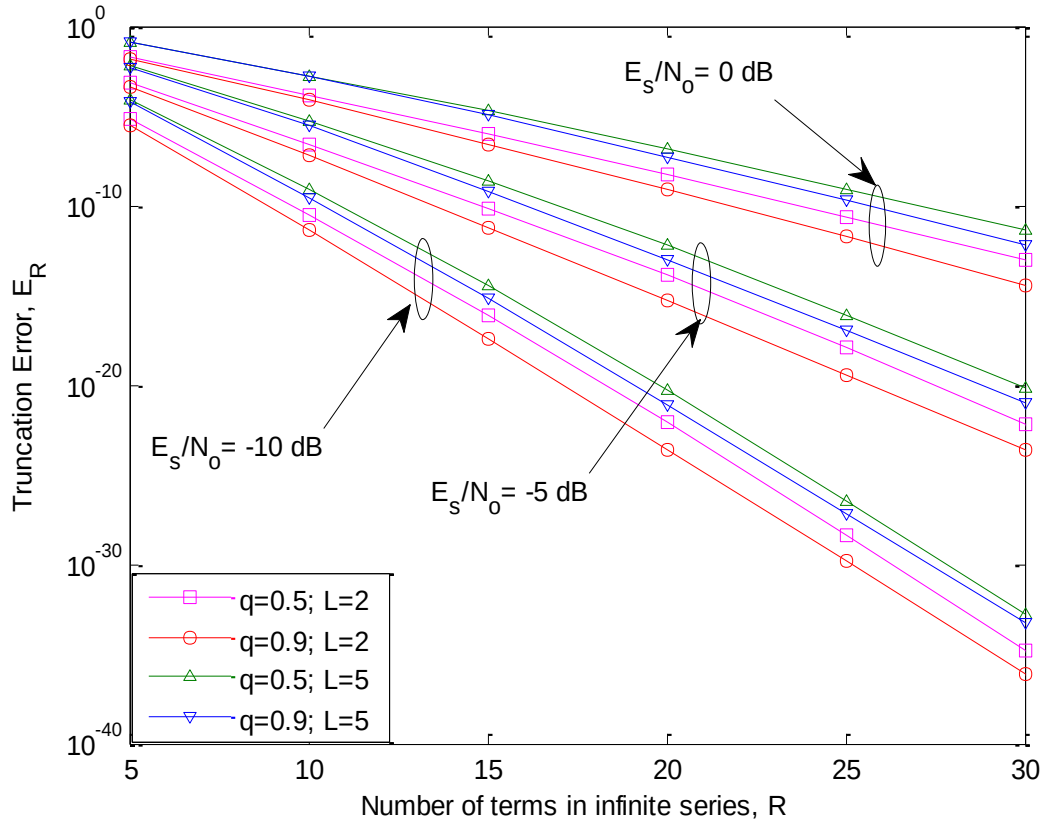

Figure 5.8 Truncation error for AUC as a function of R with different combination of system parameters for L-Hoyt/lognormal channel

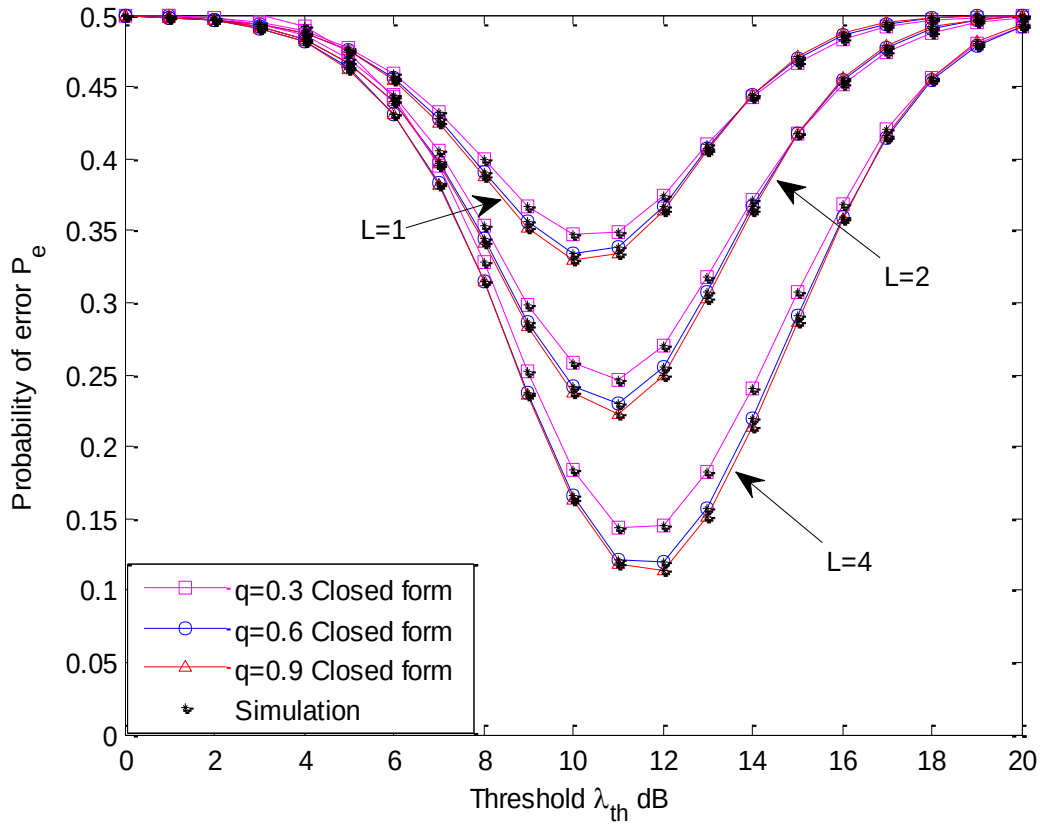

Figure 5.9 Probability of error curve as a function of threshold with several values of q and L for L-Hoyt/gamma channel

Figure 5.8 depicts the truncation error as a function of the number of terms in infinite series, *R*. The upper bound on the truncation error for AUC in equation 5.18 has been obtained. It can be observed that the error bound decreases very fast with *R*. It is clear from the plots that more number of terms is required for higher diversity order to achieve the desired accuracy. In Figure 5.9, the probability of error is depicted as a function of detection threshold. It is observed that P_e is lowest for a single value of detection threshold, and start increasing when we move away from optimum detection threshold. It is noted that when we move from *L*=1 to *L*=4, the gap is more between the plots of the different fading parameters, clearly indicating more improvement in system performance

Table 5.1 MSE for convergence of the equations (5.3), (5.7) and (5.8) for various values of N and diversity order for L-Hoyt/gamma channel

Performance Parameters	L = 1			L = 4		
	N=3	N=5	N=10	N=3	N=5	N=10
$\overline{P_D}$ (5.3)	1.1945×10^{-10}	4.5106×10^{-12}	7.2042×10^{-16}	8.3760×10^{-8}	5.7983×10^{-9}	2.6168×10^{-12}
$\overline{A}$ (5.7)	9.3275×10^{-8}	1.3217×10^{-9}	3.2167×10^{-14}	1.7124×10^{-6}	3.6219×10^{-8}	4.2981×10^{-11}
P_e (5.8)	3.6580×10^{-6}	4.6064×10^{-8}	1.0919×10^{-12}	4.8765×10^{-4}	9.5908×10^{-6}	1.7603×10^{-9}

for higher values of q. In Table 5.1, MSE incurred in truncating the infinite series of equations (5.3), (5.7) and (5.8) for various values of N and diversity order has been numerically evaluated. From the Table, it can be noted that MSE decreases with the increase in N and increases with the increase in L. The convergence rate of the series has been observed to be fast and hence the computation time is not significant.

5.4 Significance Findings

The performance of energy detector over L-Hoyt/gamma and L-Hoyt/lognormal composite fading channel is investigated. The analytical expressions of average probability of detection and average area under the receiver operating characteristic are evaluated. Further, we have optimized the detection threshold parameter by minimizing the probability of error. All the results produced here are compared with the Monte-Carlo/Exact simulations. The analytical results produced here can be useful in several wireless applications where multipath and shadowing are characterized by Hoyt/lognormal distribution.

This chapter is based on the following works:

Sandeep Kumar, *Pappu Kr. Verma, Manpreet Kaur, Sanjay Kumar Soni, Priyanka Jain, "Performance Evaluation of Energy Detection over Hoyt/gamma Channel with MRC Reception", Journal of Electromagnetic Waves and Applications, 2018, (accepted).* ***(Taylor & Francis, Impact factor – 0.864)*** [**114**]

Sandeep Kumar, *Sanjay Kumar Soni, Priyanka, "Performance of MRC receiver over Hoyt/lognormal Composite Fading Channel", International Journal of Electronics, 2018, 105(9),1433-1450 DOI: https://doi.org/10.1080/00207217.2018.1460870,* ***(Taylor & Francis, Impact factor – 0.939)*** [**112**]

CHAPTER 6

CONCLUSION AND FUTURE SCOPE OF WORK

In this dissertation, performance evaluation of composite fading channels has been performed. The closed-form expressions of the performance parameters are evaluated and analysed. Mathematical model analysis always seeks for closed-form expression. The closed-form expressions of the performance parameters are very useful in comparison to the original integral expressions. Closed-form expressions are usually evaluated instantly and provide insightful information about the context of a problem. More appropriately, we can predict the impact of parameters by looking at the equation. The closed-form solution are useful to predict the performance of the system before deploying it (saves time and money). They also help in knowing what the best modulation is scheme/order, required SNR, etc. to achieve the target performance. Closed form expressions may reduce the implementation complexity and computational cost of the system. They may be incorporated into planning software packages, etc. In this chapter, the major contributions, achievements, and future scope of work of the thesis are summarized.

6.1 Conclusion

Focusing on the analytical approach, mathematical expressions for various performance measures have been obtained. The PDF-based approach is used in all the analysis for these performance measures. The mathematically obtained expressions are numerically

evaluated and the effect of different system parameters on the receiver performance is studied. The numerical results have been validated with the Monte-Carlo simulations results. The main conclusions of this thesis are summarised as follows:

- Taking note of the fact that Hoyt is known to capture the severe multipath fading and gamma distribution is most widely used to model shadowing, we have analyzed the performance of *L*-Hoyt/gamma composite fading model. Closed-form expressions for PDF of instantaneous SNR, outage probability, AF, channel capacity and ASEP/ABEP of the composite *L*-Hoyt/gamma were obtained in terms of generalized hypergeometric functions and the corresponding results are demonstrated. The effect of diversity on the receiver performance is discussed. These expressions can be useful in the performance evaluation of *L*-Hoyt/gamma composite fading environment.
- The performance of energy detector over *L*-Hoyt/gamma fading channel has been analyzed. The analytical expressions of average probability of detection and average AUC are evaluated. Further, we have optimized the detection threshold by minimizing the total probability of error. The performance of energy detector can be improved at low SNR by using optimized threshold. Moreover, the effect of diversity on the performance of energy detector is discussed. The derived results are useful for system design engineers and can be directly used in several wireless applications such as cooperative and non-cooperative CR networks.
- The closed form PDF expression for *L*-Hoyt/lognormal composite fading channel using mixture gamma distribution has been derived. Performance metrics, such asP_{out}, AF, channel capacity and ASEP/ABEP for different

modulation schemes, were expressed in closed form. We have also presented accurate analytical expressions for the average probability of detection and average AUC. The impact of system parameters on the performance of energy detector is studied in terms of CROC and average AUC. Further, the detection threshold parameter is optimized by minimizing the probability of error for *L*-Hoyt/lognormal channel. The analytical results produced here can be useful in several wireless applications where multipath and shadowing are characterized by Hoyt/lognormal distribution.

The obtained expressions for performance measures are obtained in terms of gamma, incomplete gamma and hypergeometric functions. All the computations and simulations are carried out in MATLAB (version R2014a).

6.2 Future Scope of Work

This thesis has addressed different problems that are related to performance analysis of fading channels and energy detector based SS for CR. However, there are also other questions, which are being currently investigated and which have not been presented in this thesis. This research work gives rise to several possible improvements and future research directions.

- The behavior of an energy detector over multipath/shadowing fading channels with diversity reception was extensively analyzed in this thesis. Further analysis for the performance of an energy detector over composite generalized multipath/shadowing fading with diversity reception and for co-channel interference can be considered.

- In [**115**], α–η-κ–μ fading model is proposed that accounts for virtually all relevant short-term propagation phenomena described in the literature. The statistics of α–η-κ–μ distribution and its combination with shadowing models can be investigated. Moreover, these expressions can be utilized to evaluate the performance of energy detector over the said channels.
- The micro-diversity analysis of composite fading channels has been investigated in this thesis for studying the performance of an energy detector. Nevertheless, this type of study has not yet been performed for other SS techniques such as CFD as well as for MFD.

BIBLIOGRAPHY

[1] M. K. Simon and M. S. Alouini, *Digital Communications over Fading Channels: A Unified Approach to Performance Analysis*, 2nd ed. NY: John Wiley & Sons, 2004.

[2] P. M. Shankar, *Fading and shadowing in wireless systems*, 1st ed. NY: Springer, 2012.

[3] T. S. Rappaport, *Wireless Communications: Principles and Practice*, 2nd ed.: Prentice Hall, 2001.

[4] M. Schwartz, W. R. Bennett, and S. Stein, *Communication Systems and Techniques*. NY: McGraw-Hill, 1966.

[5] M. S. Alouini and A. J. Goldsmith, "A unified approach for calculating error rates of linearly modulated signals over generalized fading channels," *IEEE Transactions on Communications*, vol. 47, no. 9, pp. 1324-1334, Sep. 1999.

[6] S. R. McConoughey et al., "Coverage prediction for mobile radio systems operating in the 800/900 MHz frequency range," *IEEE Transactions on Vehicular Technology*, vol. 37, no. 1, pp. 3-72, Feb 1988.

[7] R. Singh, S. K. Soni, R. S. Raw, and S. Kumar, "A New Approximate Closed-Form Distribution and Performance Analysis of a Composite Weibull/Log-Normal Fading Channel," *Wireless Personal Communications*, vol. 92, no. 3, pp. 883-900, 2017.

[8] A. Abdi and M. Kaveh, "K distribution: an appropriate substitute for Rayleigh-lognormal distribution in fading-shadowing wireless channels," *Electronics Letters*, vol. 34, no. 9, pp. 851-852, Apr 1998.

[9] J. Karmeshu and R. Agrawal, "On efficacy of Rayleigh-inverse Gaussian distribution over K-distribution for wireless fading channels," *Wireless Communications & Mobile Computing*, vol. 7, no. 1, pp. 1–7.

[10] A. Laourine, M. S. Alouini, S. Affes, and A. Stephenne, "On the performance analysis of composite multipath/shadowing channels using the G-distribution," *IEEE Transactions on Communications*, vol. 57, no. 4, pp. 1162-1170, Apr 2009.

[11] J. G. Proakis and M. Salehi, *Fundamentals of Communication Systems*, 1st ed.: Pearson Education, 2004.

[12] J. G. Proakis, *Digital Communications*, 5th ed. NY: McGraw-Hill, 2008.

[13] G. L. Stüber, *Principles of Mobile Communications*, 2nd ed.: Springer, 2000.

[14] A. Goldsmith, *Wireless Communications*, 5th ed.: Cambridge University Press, 2005.

[15] J. Mitola and G. Q. Maguire, "Cognitive radio: making software radios more personal," *IEEE Personal Communications*, vol. 6, no. 4, pp. 13-18, Aug 1999.

[16] S. Haykin, "Cognitive radio: brain-empowered wireless communications," *IEEE Journal on Selected Areas in Communications*, vol. 23, no. 2, pp. 201-220, Feb

2005.

[17] D. Borth, R. Ekl, B. Oberlies, and S. Overby, "Considerations for Successful Cognitive Radio Systems in US TV White Space," in *IEEE Symposium on New Frontiers in Dynamic Spectrum Access Networks*, vol. 3rd, Chicago, 2008, pp. 1-5.

[18] T. Yucek and H. Arslan, "A survey of spectrum sensing algorithms for cognitive radio applications," *IEEE Communications Surveys & Tutorials*, vol. 11, no. 1, pp. 116-130, 2009.

[19] V. K. Bhargava and E. Hossain, *Cognitive Wireless Communication Networks*. NY: Springer, 2007.

[20] T. Haiyun, "Some physical layer issues of wide-band cognitive radio systems," in *IEEE International Symposium on New Frontiers in Dynamic Spectrum Access Networks*, Baltimore, MD, USA, 2005, pp. 151-159.

[21] H. Urkowitz, "Energy detection of unknown deterministic signals," *Proc. IEEE*, vol. 55, no. 4, pp. 523-531, Apr. 1967.

[22] H. Urkowitz, "Energy detection of unknown deterministic signals," *IEEE*, vol. 55, no. 4, pp. 523-531, Apr 1967.

[23] F. F. Digham, M. S. Alouini, and M. K. Simon, "On the Energy Detection of Unknown Signals Over Fading Channels," *IEEE Transactions on Communications*, vol. 55, no. 1, pp. 21-24, Jan 2007.

[24] I. S. Gradshteyn and I. M. Ryzhik, *Table of Integrals, Series, and Products*, 6th ed. NY: Academic Press, 2000.

[25] W. C. Jakes, *Microwave mobile communication*, 2nd ed. NJ, Piscataway: IEEE Press , 1994.

[26] J. Salo, H. M. El-Sallabi, and P. Vainikainen, "The distribution of the product of independent Rayleigh random variables," *IEEE Transactions on Antennas and Propagation*, vol. 54, no. 2, pp. 639-643, Feb. 2006.

[27] B. Talha and M. Patzold, "On the statistical properties of double Rice channels," in *International Symposium on Wireless Personal Multimedia Communications*, Jaipur, India, 2007, pp. 517-522.

[28] J. R. Mendes and M. D. Yacoub, "A General Bivariate Ricean Model and Its Statistics," *IEEE Transactions on Vehicular Technology*, vol. 56, no. 2, pp. 404-415, Mar. 2007.

[29] N. C. Sagias, D. A. Zogas, G. K. Karagiannidis, and G. S. Tombras, "Channel capacity and second-order statistics in Weibull fading," *IEEE Communications Letters*, vol. 8, no. 6, pp. 377-379, Jun. 2004.

[30] F. El Bouanani, H. Ben-Azza, and M. Belkasmi, "New Results for the Shannon channel capacity over generalized multipath fading channels for MRC diversity," *EURASIP Journal on Wireless Communications and Networking*, vol. 2012, pp. 1-12, 2012.

[31] N. Youssef, W. Elbahri, M. Patzold, and S. Elasmi, "On the crossing statistics of phase processes and random FM noise in Nakagami-q mobile fading channels," *IEEE Transactions on Wireless Communications*, vol. 4, no. 1, pp. 24-29, Jan. 2005.

[32] J. F. Paris, "Nakagami-q (Hoyt) distribution function with applications," *Electronics Letters*, vol. 45, no. 4, pp. 210-212, Feb. 2009.

[33] J. F. Paris and D. Morales-Jimenez, "Outage probability analysis for Nakagami-q (Hoyt) fading channels under Rayleigh interference," *IEEE Transactions on Wireless Communications*, vol. 9, no. 4, pp. 1272-1276, Apr. 2010.

[34] R. M. Radaydeh, "Performance of Cellular Mobile Systems Employing SNR-Based GSC in the Presence of Rayleigh and Nakagami-q Cochannel Interferers," *IEEE Transactions on Vehicular Technology*, vol. 58, no. 6, pp. 3081-3088, Jul. 2009.

[35] S. Krithiga and V. Bhaskar, "Capacity and BER performance of independent and identically distributed a-u fading channel under absolute SNR scheduling," in *IEEE Int. Conf. Commun. Sig. Process.*, 2013, pp. 387-391.

[36] A. Abdi, K. Wills, H. A. Barger, M. S. Alouini, and M. Kaveh, "Comparison of the level crossing rate and average fade duration of Rayleigh, Rice and Nakagami fading models with mobile channel data," in *IEEE Vehicular Technology Conference*, Boston, 2000, pp. 1850-1857.

[37] F. Heliot, M. Ghavami, and M. R. Nakhai, "An accurate closed-form

approximation of the average probability of error over a log-normal fading channel," *IEEE Transactions on Wireless Communications*, vol. 7, no. 5, pp. 1495-1500, May 2008.

[38] V. Khandelwal and Karmeshu, "A New Approximation for Average Symbol Error Probability over Log-Normal Channels," *IEEE Wireless Communications Letters*, vol. 3, no. 1, pp. 58-61, Feb 2014.

[39] Khandelwal and V. Karmeshuand, "On the applicability of average channel capacity in log-normal fading environment," *Wireless Personal Communications*, vol. 68, no. 4, pp. 1393–1402, Feb 2013.

[40] S. L. Cotton and W. G. Scanlon, "Higher Order Statistics for Lognormal Small-Scale Fading in Mobile Radio Channels," *IEEE Antennas and Wireless Propagation Letters*, vol. 6, pp. 540-543, 2007.

[41] P. S. Bithas, N. C. Sagias, P. T. Mathiopoulos, G. K. Karagiannidis, and A. A. Rontogiannis, "On the performance analysis of digital communications over generalized-K fading channels," *IEEE Communications Letters*, vol. 10, no. 5, pp. 353-355, May 2006.

[42] P. S. Bithas, "Weibull-gamma composite distribution: alternative multipath/shadowing fading model," *Electronics Letters*, vol. 45, no. 14, pp. 749-751, Jul 2009.

[43] P. M. Shankar, "An overview of shadowed fading wireless channels in terms of a

cascaded approach," *Physical Communication*, pp. 59-65, Jun 2015.

[44] P. M. Shankar, "A Nakagami-N-gamma Model for Shadowed Fading Channels," *Wireless Personal Communications*, vol. 64, no. 4, pp. 665-680, Jun 2012.

[45] F. Hansen and F. I. Meno , "Mobile fading; Rayleigh and lognormal superimposed," *IEEE Vehicular Technology*, vol. 26, no. 4, pp. 332–335, Nov. 1977.

[46] F. Vatalaro, "Generalised Rice-lognormal channel model for wireless communications," *Electronics Letters*, vol. 31, no. 22, pp. 1899–1900, Oct. 1995.

[47] E. K. Al-Hussaini, A. M. Al-Bassiouni, H. M. Mouradand, and H. Al-Shennawy, "Composite macroscopic and microscopic diversity of sectorized macro cellular and microcellular mobile radio systems employing RAKE receiver over Nakagami fading plus lognormal shadowing channel," *Wireless Personal Communications*, vol. 21, no. 3, pp. 309–328, Jun. 2002.

[48] S. Atapattu, C. Tellambura, and H. Jiang, "Representation of composite fading and shadowing distributions by using mixtures of Gamma Distributions," in *IEEE Wireless Commuinication and Networking Conference*, Sydney, Australia, 2010, pp. 1-5.

[49] A. M. Mitic and M. M. Jakovljevic, "Second-order statistics in Weibull-lognormal fading channels," in *International Conference on Telecommunications in Modern Satellite, Cable and Broadcasting Services*, Nis, 2007, pp. 529-532.

[50] A. Abdi and M. Kaveh, "Comparison of DPSK and MSK bit error rates for K and Rayleigh-lognormal fading distributions," *Communications Letters IEEE* , vol. 4, no. 4, pp. 122–124, 2000.

[51] J. Zhang, M. Matthaiou, Z. Tan, and H. Wang, "Performance analysis of digital communication systems over composite n-u/gamma fading channels," *IEEE Transactions on Vehicular Technology*, vol. 61, no. 7, pp. 3114-3124, Sep 2012.

[52] Z. Lingwen, Z. Jiayi, and L. Liu, "Average channel capacity of k-u/gamma fading channels," *China Commun.*, vol. 10, no. 6, pp. 28-34, Jun 2013.

[53] C. García-Corrales, F. J. Cañete, and J. F. Paris, "Capacity of k-u Shadowed Fading Channels," *International Journal of Antennas and Propagation*, vol. 2014, pp. 1-8, Jul. 2014.

[54] E. J. Leonardo and M. D. Yacoub, "The product of two a-u variates and the composite a-u multipath-shadowing Model," *IEEE Transactions on Vehicular Technology*, vol. 64, no. 6, pp. 2720-2725, Jun. 2015.

[55] N. Y. Ermolova and O. Tirkkonen, "Outage probability over composite n-u fading-shadowing radio channels," *IET Communications*, vol. 6, no. 13, pp. 1898-1902, Sep 2012.

[56] P. M. Shankar, "Statistical Models for Fading and Shadowed Fading Channels in Wireless Systems: A Pedagogical Perspective," *Wireless Personal Communications*, vol. 60, no. 2, pp. 191-213, Sep. 2011.

[57] C. D. Iskander and P. T. Mathiopoulos, "Exact Performance Analysis of Dual-Branch Coherent Equal-Gain Combining in Nakagami-m, Rice and Hoyt Fading," *IEEE Transactions on Vehicular Technology*, vol. 57, no. 2, pp. 233–239, Mar 2008.

[58] A. Baid, H. Fadnavis, and P. R. Sahu, "Performance of a prediction EGC receiver in Hoyt fading channel for arbitrary number of branches," *IEEE Communication Letters*, vol. 12, no. 9, pp. 627-629, Sep. 2008.

[59] R. M. Radaydeh and M. M. Matalgah, "Average BER analysis of M-ary FSK signal in Nakagami-q(Hoyt) fading with non coherent diversity combining," *IEEE Transactions on Vehicular Technology*, vol. 57, no. 4, pp. 2257-2267, Jul. 2008.

[60] D. A. Zogas, G. K. Karagiannidis, and S. A. Kotsopoulos, "Equal gain combining over Nakagami-n (Rice) and Nakagami-q (Hoyt) generalized fading channels," *IEEE Transactions on Wireless Communications*, vol. 4, no. 2, pp. 374–379, Mar. 2005.

[61] A. C. Moraes, D. B. da Costa, and M. D. Yacoub, "An outage analysis of multibranch diversity receivers with cochannel interference in a-u, n-u and k-u fading scenarios," *Wireless Pers. Commun.*, vol. 64, no. 1, pp. 3-19, Jan. 2012.

[62] Y. Chen. and C. Tellambura, "Performance analysis of three branch selection combining over arbitrary correlated Rayleigh fading channels," *IEEE Transactions on Wireless Communications*, vol. 4, no. 3, pp. 861-865, May 2005.

[63] Y. Chen and C. Tellambula, "Distribution functions of selection combiner output in equally correlated Rayleigh, Rician, and Nakagami-m fading channels," *IEEE Transactions on Communications*, vol. 52, no. 11, pp. 1948-1956, Nov. 2004.

[64] J. Reig, V. M. Rodrigo Pe narrocha, and L. Rubio, "Performance of dual selection combiners over correlated nakagami-m fading with different fading parameters," *IEEE Trans. Commun.*, vol. 54, no. 9, pp. 1527-1532, 2006.

[65] M. Uysal, "Maximum achievable diversity order for cascaded Rayleigh fading channels," *Electronics Letters*, vol. 41, no. 23, pp. 1289–1290, 2005.

[66] W. Wongtrairat and P. Supnithi, "Performance of Digital Modulation in Double Nakagami-m Fading Channels with MRC Diversity," *Communications IEICE*, no. 2, pp. 559–566, 2009.

[67] G. K. Karagiannidis, "Performance analysis of triple selection diversity over exponentially correlated Nakagami- m fading channels," *Communications IEEE*, vol. 51, no. 8, pp. 1245–1248, 2003.

[68] S. Khatalin and J. P. Fonseka, "On the channel capacity in Rician and Hoyt fading environments with MRC diversity," *IEEE Trans. Veh. Technol.*, vol. 55, pp. 137-141, Jan 2006.

[69] R. Subadar and P. R. Sahu, "Performance of L-MRC receiver over independent Hoyt fading channels," in *National Conference on communications*, Chennai, 2010, pp. 1–5.

[70] G. A. Ropokis, A. A. Rontogiannis, and P. T. Mathiopoulos, "Performance analysis of orthogonal space-time block coding over Hoyt fading channels," in *Globecom*, 2007, pp. 3416-3420.

[71] D. Morales-Jimenez, J. F. Paris, and A. Lozano, "Outage probability analysis for MRC in n-u fading channels with co-channel interference," *IEEE Commun. Lett*, vol. 16, no. 5, pp. 674-677, May 2012.

[72] M. M. El Ayadi and M. H. Ismail, "Novel closed-form exact expressions and asymptotic for the symbol error rate of single- and multiple-branch MRC and EGC receivers over a-u fading," *IEEE Transaction on Vehicular Technology*, vol. 63, no. 9, pp. 4277-4291, Nov. 2014.

[73] J. Jung, S. R. Lee, H. Park, S. Lee, and I. Lee, "Capacity and error probability analysis of diversity reception schemes over generalized-K fading channels using a mixture gamma distribution," *IEEE Trans. Wireless Commun.*, vol. 13, no. 9, pp. 4721-4730, Sep 2014.

[74] R. Singh, S. K. Soni, P. K. Verma, and S. Kumar, "Performance Analysis of MRC Combiner Output in Log Normal Shadowed Fading," in *IEEE International Conference on Computing,Communication and Automation*, 2015.

[75] A. Laourine and A. Stephenne, "Estimating the ergodic capacity of log-normal channels," *Communications Letters IEEE*, vol. 11, no. 7, pp. 568–570.

[76] M. Safari and M. Uysal, "Cooperative diversity over log-normal fading channels:

performance analysis and optimization," *IEEE Transactions on Wireless Communications*, vol. 7, no. 5, pp. 1963-1972, May 2008.

[77] Alouini, M. S. Alouini, and M. K. Simon, "Dual diversity over correlated log-normal fading channels," *IEEE Transactions on Communications*, vol. 50, no. 12, p. Dec., D 2002.

[78] C. Stefanovic, B. Jaksic, P. Spalevic, S. Panic, and Z. Trajcvski, "Performance analysis of selection combining over correlated Nakagami-m fading channels with constant correlation model for desired signal and co-channel interference," *Radioengineering*, vol. 22, no. 4, pp. 1176–1181, 2013.

[79] A. S. Panajotovic, "Effect of Microdiversity and Macrodiversity on Average Bit Error Probability in Shadowed Fading Channels in the Presence of Interference," *ETRI Journal*, vol. 31, no. 5, pp. 500–505, 2009.

[80] B. Jaksic, D. Stefanovic, M. Stefanovic, P. Spalevic, and V. Milenkovic, "Level crossing rate of macrodiversity system in the presence of multipath fading and shadowing," *Radioengineering*, vol. 24, no. 1, pp. 185–191, 2015.

[81] S. Atapattu, C. Tellambura, and H. Jiang, "MGF based analysis of area under the ROC curve in energy Detection," *IEEE Commun. Lett.*, vol. 15, no. 12, pp. 1301-1303, Dec 2011.

[82] S. Atapattu, C. Tellambura, and H. Jiang, "Energy detection of primary signals over n-u fading channels," in *IEEE International Conference on Industrial and*

Information Systems (ICIIS), Sri Lanka, 2009, pp. 118-122.

[83] H. Al - Hmood and H. S. Al-Raweshidy, "Performance analysis of energy detector over η − μ fading channel," *Electronics Letters*, vol. 51, no. 3, pp. 249-251, 2015.

[84] Y. Fathi and M. H. Tawfik, "Versatile performance expression for energy detector over α−μ generalised fading channels," *Electronics Letters* , vol. 48, no. 17, pp. 1081–1082, 2012.

[85] P. C. Sofotasios et al., "Energy detection based spectrum sensing over κ − μ and κ − μ extreme fading channels," *IEEE Transaction on Vehicular Technology*, vol. 62, no. 3, pp. 1031–1040, 2013.

[86] S. Singh and S. Sharma , "Performance analysis of spectrum sensing techniques over TWDP fading channels for CR based IoTs," *Electronics and Communications* , vol. 80, pp. 210-217, 2017.

[87] H. Rasheed, F. Haroon , and N. Rajatheva, "Performance of Rice-lognormal channel model for spectrum sensing," in *IEEE international conference on electrical engineering/electronics computer telecommunication and information technology*, 2010, pp. 420-424.

[88] S. Atapattu, C. Tellambura, and H. Jiang, "Performance of an energy detector over channels with both multipath fading and shadowing," *IEEE Transactions on Wireless Communications*, vol. 9, no. 12, pp. 3662-3670, 2010.

[89] H. Rasheed, F. Haroon, and F. Adachi, "On the energy detection over generalized-k (KsubGsub) fading," in *IEEE 14th INMIC*, 2011, pp. 367-371.

[90] K. P. Peppas, G. Efthymoglou, V. A. Aalo, M. Alwakeel, and S. Alwakeel, "Energy detection of unknown signals in Gamma-shadowed Rician fading environments with diversity reception," *IET communications*, vol. 9, no. 2, pp. 196-210, 2015.

[91] H. Al-Hmood and H. S. Al-Raweshidy, "Unified Modeling of Composite k−μ/Gamma, η−μ/Gamma and α−μ/Gamma Fading Channel Using a Mixture Gamma Distribution with Applications to Energy Detection," *IEEE Antennas and Wireless Propagation Letters*, vol. 16, pp. 104-108, 2016.

[92] S. P. Herath and N. Rajatheva, "Analysis of equal gain combing in energy detection for cognitive radio over Nakagami channels," in *IEEE Global Communication Conference (GLOBECOM)*, 2008, pp. 1-5.

[93] S. Attapattu, C. Tellambura, and H. Jiang, "Analysis of area under the ROC curve of energy detection," *IEEE Transactions on Wireless Communication*, vol. 9, no. 3, pp. 1216-1225, 2010.

[94] Shahini, A. Bagheri, and A. Shahzadi, "A unified approach to performance analysis of energy detection with diversity receivers over Nakagami-m fading channels," in *IEEE Int. Conf. Connected Veh. and Expo (ICCVE)*, 2013, pp. 707-712.

[95] S. P. Herath, N. Rajatheva, and C. Tellambura, "Energy detection of unknown

signals in fading and diversity reception," *IEEE Transaction on Communications*, vol. 59, no. 9, pp. 2443-2453, 2011.

[96] J. P. Peña-Martín, J. M. Romero-Jerez, and C. Tellez-Labao, "Performance of selection combining diversity in η − μ fading channels with integer values of μ," *IEEE Transaction on Vehicular Technology*, vol. 64, no. 2, pp. 834–839., 2015.

[97] Annamalai and A. Olaluwe, "Energy detection of unknown deterministic signals in k-u and n-u generalized fading channels with diversity receivers," in *IEEE Computing Net. Commun. (ICNC)*, 2014, pp. 761-765.

[98] E. Adebola and A. Annamalai, "Unified analysis of energy detectors with diversity reception in generalised fading channels," *IET Communications*, vol. 8, no. 17, pp. 3095–3104, 2014.

[99] H. Al-Hmood and H. S. Al-Raweshidy, "Analysis of energy detection with diversity receivers over non-identically distributed κ − μ shadowed fading channels," *Electronics Letters*, vol. 53, no. 2, pp. 83-85, 2017.

[100] W. Zhang and K. B. Letaief, "Cooperative spectrum sensing with transmit and relay diversity in cognitive radio networks," *IEEE Trans. Wireless Commun.*, vol. 7, no. 12, pp. 4761-4766, 2008.

[101] G. Chandrasekaran and S. Kalyani , "Performance analysis of cooperative spectrum sensing over κ − μ shadowed fading," *IEEE Wireless Communications Letters*, vol. 4, no. 5, pp. 553–556, 2015.

[102] J. Li , B. Li , and M. Liu, "Performance analysis of cooperative spectrum sensing over large and small scale fading channels," *International Journal of Electronics and Communication*, vol. 78, pp. 90-97, 2017.

[103] N. Wang, Y. Gao, and X. Zhang, "Adaptive spectrum sensing algorithm under different primary user utilizations," *IEEE communications letters*, vol. 17, no. 9, pp. 1838-1841, 2013.

[104] S. Zhang and Z. Bao, "An adaptive spectrum sensing algorithm under noise uncertainty," in *IEEE International Conference on Communications*, 2011, pp. 1-5.

[105] A. Kozal, M. Merabti, and F. Bouhafs, "An improved energy detection scheme for cognitive radio networks in low SNR region," in *IEEE International symposium on Computers and Communications*, 2012, pp. 684-689.

[106] S. Atapattu, C. Tellambura, and H. Jiang, "Spectrum sensing via energy detector in low SNR," in *IEEE Int. Conf. Commun. (ICC)*, 2011, pp. 1-5.

[107] Wolfram. (2017, Dec.) Wolfram function site. [Online]. http://functions.wolfram.com/PDF/MeijerG.pdf

[108] O. Olabiyi and A. Annamalai, "Invertible exponential-type approximations for the Gaussian probability integral Q(x) with applications," *IEEE Wireless Communications Letters*, vol. 1, no. 5, pp. 544–547, 2012.

[109] M. K. Simon and M. S. Alouini, "A unified approach to the probability of error for non-coherent and differentially coherent modulations over generalized fading

channels," *IEEE Transactions on Communications*, vol. 46, no. 12, pp. 1625–1638, 1996.

[110] S. Kumar, S. Soni, and P. Jain, "Micro-Diversity Analysis of Error Probability and Channel Capacity over Hoyt/Gamma Fading," *Radioengineering*, vol. 26, no. 4, pp. 1096-1103, 2017.

[111] Z. Wang and G. B. Giannakis , "A Simple and General Parameterization Quantifying Performance in Fading Channels," *IEEE Transaction on Communications*, vol. 51, no. 8, pp. 1389-1398, 2003.

[112] S. Kumar, S. Soni, and P. Jain, "Performance of MRC receiver over Hoyt-lognormal Composite Fading Channel," *International Journal of Electronics*, 2018.

[113] A. P. Prudnikov , Y. A. Brychkov, and O. Marichev, *Integrals and Series Volume 2, Special Functions*, 1st ed. Amsterdam: Gordon and Breach Science Publishers, 1986.

[114] S. Kumar, P. K. Verma, M. Kaur, S. K. Soni, and P. Jain, "Performance Evaluation of Energy Detection over Hoyt/Gamma Channel with MRC Reception," *Journal of Electromagnetic Waves and Applications*, vol. accepted, 2018.

[115] M. D. Yacoub, "The α–η-κ–μ Fading Model," *IEEE Transactions on Antennas and Propagation*, vol. 64, no. 8, pp. 3597-3610, 2016.

AUTHOR BIOGRAPHY

Sandeep Kumar received his B. Tech. in Electronics and Comm. from Kurukshetra University, India in 2004 and M.E. degree in Electronics and Comm. from Thapar University, Patiala, India in 2007. He is currently pursuing Ph.D. from Delhi Technological University, India. Presently he is working as Member (Senior Research Staff) at Central Research Laboratory, Bharat Electronics Ltd., Ghaziabad, India. His research interest includes the wireless channel modeling, cognitive radios, and radio network planning. He is also serving as a reviewer for various reputed journals including IEEE transaction on vehicular technology, IEEE access, International journal of electronics and communications (AEU), Wireless personal communications, Telecommunication systems and International journal of microwave and wireless technologies.

APPENDIX A

Proofs for Chapter 5

Derivation of E_R in equation 5.18

The error bound (ER) in truncating the infinite series in equation 5.17 by R number of terms is given as

$$E_R = \frac{s^L}{W}\sum_{n=0}^{\infty}\frac{t^n\left(\frac{L}{2}\right)_n}{\Gamma(L+n)n!}\sum_{k=1}^{K}w_k a_k \times\sum_{g=R}^{\infty}\frac{\Gamma(L+n+g)}{\Gamma(u)g!\Gamma(u+g+1)}\frac{\Gamma(2u+g)}{\left[1+b_k\right]^{(L+n+g)}}\,{}_2F_1(u+g,2u+g;u+g+1;-1) \tag{A.1}$$

By using the identity $a\Gamma(a)=\Gamma(a+1)$ and $a!=\Gamma(a+1)$, the above equation can be simplified as

$$E_R = \frac{s^L}{W}\sum_{n=0}^{\infty}\frac{t^n\left(\frac{L}{2}\right)_n}{\Gamma(L+n)n!}\sum_{k=1}^{K}w_k a_k \frac{1}{\left[1+b_k\right]^{(L+n+R)}}\frac{\Gamma(2u+R)\Gamma(L+n+R)}{\Gamma(u)\Gamma(R+1)\Gamma(u+R+1)} \times\sum_{l=0}^{\infty}\frac{(1)_l(L+n+R)_l(2u+R)_l}{l!(R+1)_l(u+R+1)_l}\left(\frac{1}{1+b_k}\right)^l {}_2F_1(u+R+l,2u+R+l;u+R+l+1;-1) \tag{A.2}$$

It is noted that ${}_2F_1(.,;.,;.)$ is a monotonically decreasing function for all positive values of *u, R and l.* Therefore, equation B.2 can be upper bounded as

$$E_R \le \frac{s^L}{W}\sum_{n=0}^{\infty}\frac{t^n\left(\frac{L}{2}\right)_n}{\Gamma(L+n)n!}\sum_{k=1}^{K}w_k a_k \frac{1}{\left[1+b_k\right]^{(L+n+R)}}\frac{\Gamma(2u+R)\Gamma(L+n+R)}{\Gamma(u)\Gamma(R+1)\Gamma(u+R+1)}$$
$$\times\sum_{l=0}^{\infty}\frac{(1)_l(L+n+R)_l(2u+R)_l}{l!(R+1)_l(u+R+1)_l}\left(\frac{1}{1+b_k}\right)^l {}_2F_1(u+R,2u+R;u+R+1;-1)$$

(A.3)

Using equation (9.14.1) of [**24**] a bound for E_R can be obtained in closed form as in equation 5.18, and thus, the proof concludes.